



Figures and figure supplements

Cell type boundaries organize plant development

Monica Pia Caggiano et al

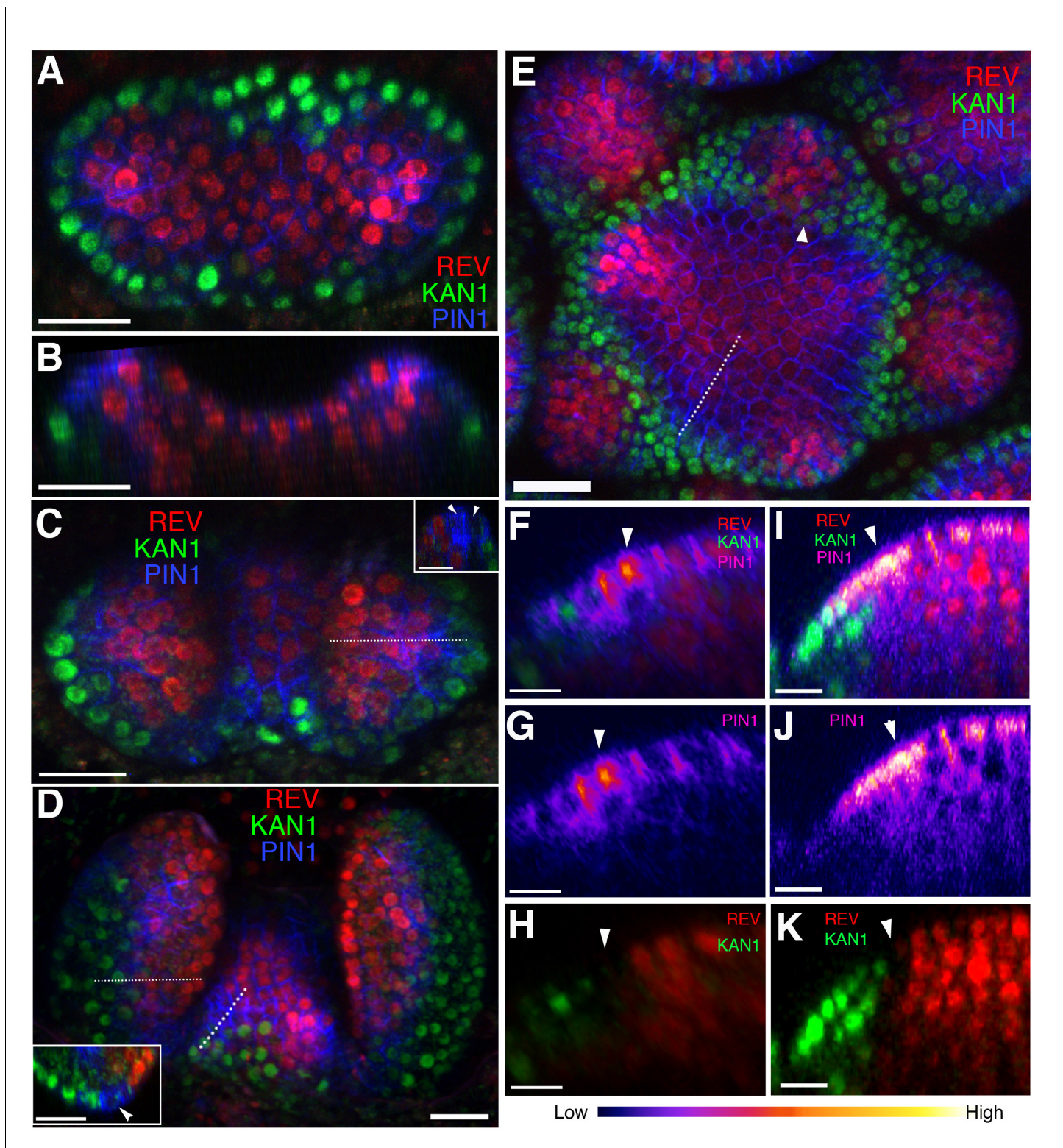


Figure 1. Organ initiation is centered on a boundary between the expression domains of genes involved in leaf dorsoventrality. (A–D) Confocal projections showing REV-2 xYPet (red), PIN1-CFP (blue) and KAN1-2 x GFP (green) expression in a vegetative shoot apical meristem at 3 days (A), 4 days (C) and 5 days (D) after stratification (DAS), respectively. Inset in (C) shows a longitudinal optical section across the dotted line in the right leaf. Inset in (D) shows a transverse optical section across the dotted line in the left leaf. White arrowheads in the insets in (C and D) mark a gap in between the REV-2 xYPet and KAN1-2 x GFP expression domains where PIN1 expression is highest. (B) Longitudinal reconstructed section of seedling shown *Figure 1 continued on next page*

Figure 1 continued

in (A). (E) Expression pattern of REV-2 \times YPet, KAN1–2 \times GFP and PIN1-CFP in an inflorescence meristem. White arrow head marks region where KAN1–2 \times GFP expression is being reestablished after floral bract emergence. (F–K) Longitudinal optical sections across the dashed lines in (D) and (E) showing localized PIN1-CFP expression (magenta) marking organ inception at the REV-2 \times YPet/KAN1–2 \times GFP boundary in both the vegetative meristem (F–H) and inflorescence meristem (I–K). White arrow heads mark cells in between the REV-2 \times YPet and KAN1–2 \times GFP expression domains where PIN1-CFP expression is highest. Scale bars, 20 μ m (A–E, inset in (D)) and 10 μ m (F–K).

DOI: <https://doi.org/10.7554/eLife.27421.002>

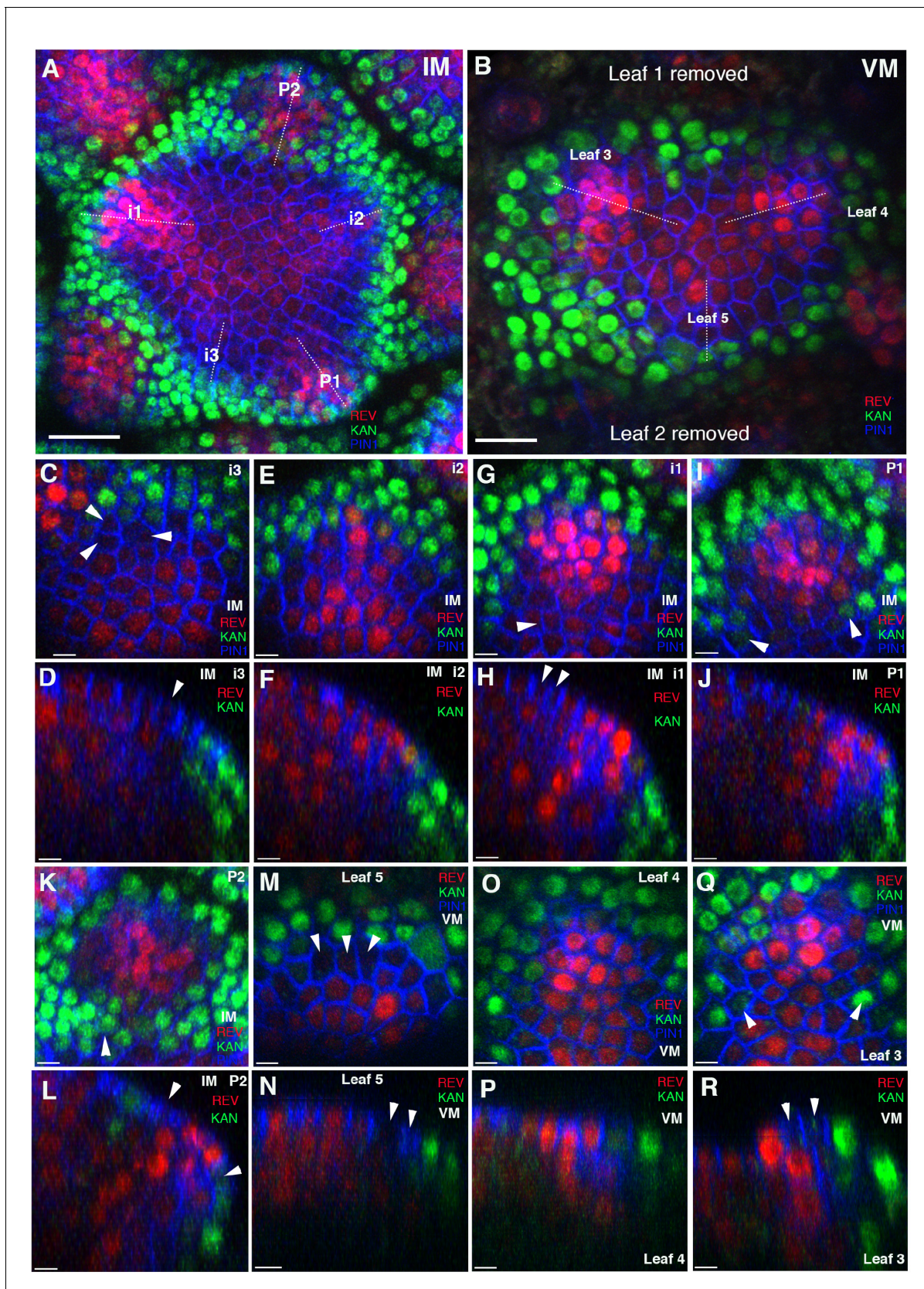


Figure 1—figure supplement 1. REV and KAN1 display dynamic expression pattern during different stages of organ development. (A and B) Confocal projections of the IM (A) (same as **Figure 1A**) and the VM of a seedling 5DAS (B) showing expression pattern of REV-2 xYPet (red), KAN1-2 x GFP (green), and PIN1 (blue). Figure 1—figure supplement 1 continued on next page

Figure 1—figure supplement 1 continued

(green) and PIN1-CFP (blue). Primordium (P) and incipient primordium (i) stages are numbered from i3-P2 in (A) based on convention described in (Heisler *et al.*, 2005). Leaves in (B) are numbered starting from oldest to youngest. (C–L) Magnified views of i3 (C), i2 (E), i1 (G), P1(I) and P2 (K) marked in (A); Longitudinal optical sections of i3 (D), i2 (F), i1 (H), P1(J) and P2 (L) along the dashed lines marked in (A) showing gradual changes in REV and KAN1 expression during different stages of floral bract development. Note the presence of a gap between REV and KAN1 expression in the youngest incipient primordium i3 (white arrowheads in (C) and (D)) and extension of REV at a later stage into the developing primordium i2 (E and F). At the next stage i1, REV expression starts to decrease in the surrounding cells (white arrowheads in (G) and (H)). At P1 stage, in the regions where PIN1 polarities have reversed away completely from the primordium, REV expression reduces further (I and J) and KAN1 expression starts to re-appear (white arrowheads in I). At the next stage P2, KAN1 expression is re-established in the vicinity of the primordium (white arrowhead in (K)), REV expression is restricted to the center of the primordium and a gap between REV and KAN1 expression re-appears (white arrowheads in L). (M–R) Magnified views of leaf 5 (M), leaf 4 (O), and leaf 3 (Q) marked in (B); Longitudinal optical sections of leaf 5 (N), leaf 4 (P), and leaf 3 (R) along the dashed lines marked in (B) showing gradual changes in REV and KAN1 expression during different stages of leaf primordium development. Again, note the presence of a gap between REV and KAN expression in the youngest leaf primordium 5 (white arrowheads in (M) and (N)) and extension of REV at a later stage into the developing primordium 4 (O and P), while KAN 1 expression appears relatively static (O and P). At a later stage, REV expression decreases adaxial to the primordium (Q and R) as KAN1 expression starts to appear (white arrowheads in Q) and a gap between REV and KAN1 expression is re-established (white arrowheads in R). Scale bars 20 μm (A), 15 μm (B) and 5 μm (C–R).

DOI: <https://doi.org/10.7554/eLife.27421.003>

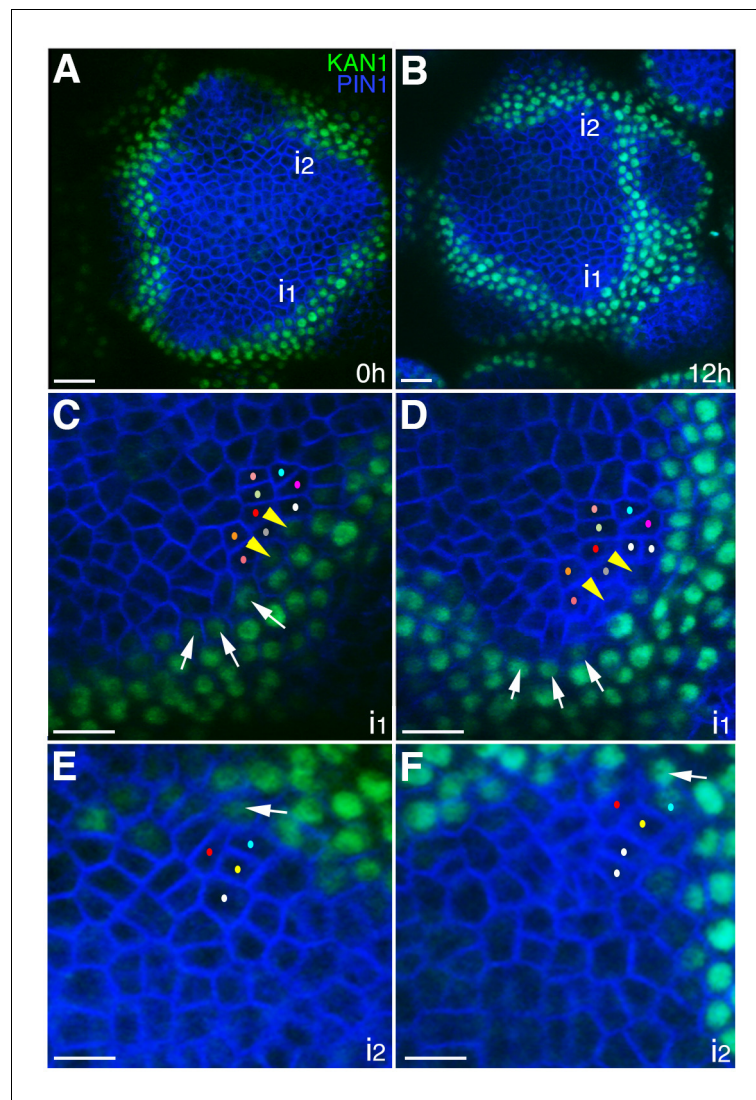


Figure 2. The expression of KAN1–2 × GFP is relatively stable with respect to the underlying cells within initiating organs. (A–B) Confocal projections showing an inflorescence meristem viewed from above expressing PIN1-CFP (blue) and KAN1–2 × GFP (green) at two time points (0 hr and 12 hr). Two incipient primordia are marked i1 and i2. (C–D) Close up views corresponding to primordium i1 from (A) and (B) with white arrows marking three cells at the edge of KAN1–2 × GFP expression that retain this expression over the time interval. Yellow arrow heads mark two cells in which KAN1–2 × GFP is absent at 12 hr. Similar colored dots mark the same cells in (C) and (D), tracked over 12 hr. (E) Close up view of primordium i2 in (A) with arrow marking adaxial edge of KAN1 expression. (F) Close up of primordium i2 in (B) showing the same cell marked in (E) remaining at the adaxial edge of KAN1 expression after 12 hr. Similar colored dots mark the same cells in (E) and (F), tracked over 12 hr. Scale bars, 20 μm in (A and B); 10 μm in (C–F).

DOI: <https://doi.org/10.7554/eLife.27421.004>

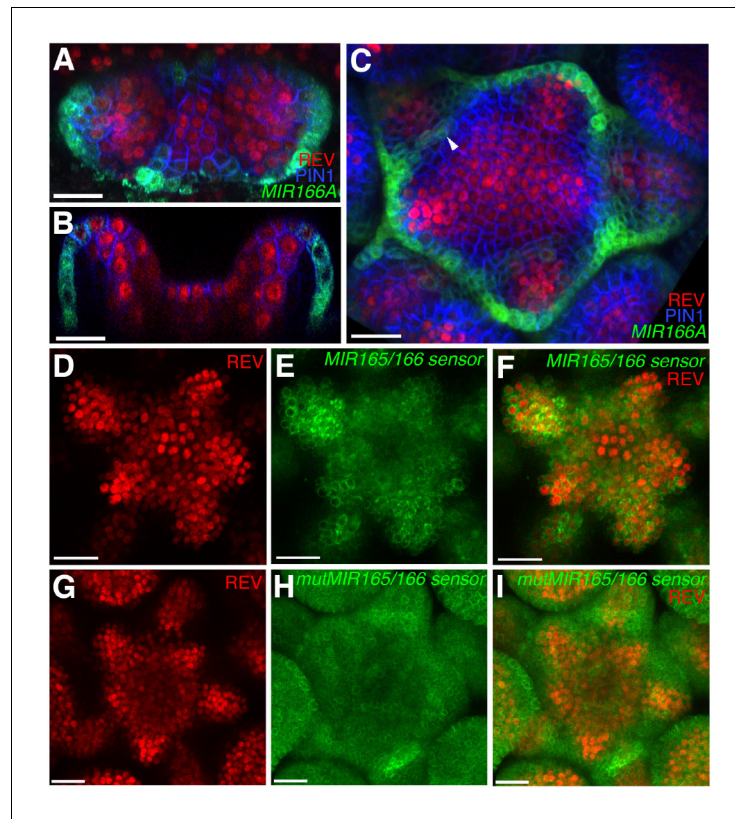


Figure 3. Expression and activity of MIR165/166 is localized to the periphery of the shoot meristem. (A) Expression of *MIR166Ap::GFPER* (green), PIN1-CFP (blue) and REV-2 × YPet (red) in the vegetative meristem (VM) at 3.5 DAS. (B) Longitudinal section of meristem shown in (A). (C) Expression of *MIR166Ap::GFPER* (green), PIN1-CFP (blue) and REV-2 × YPet (red) in the inflorescence meristem (IM). White arrow head marks the reestablishment of *MIR166Ap::GFPER* expression around the meristem after organ emergence. (D to F) Expression of REV-2 × YPet (red) alone (D), a MIR165/166 biosensor driven by the *UBQ10* promoter (green) alone (E) and both combined in the same IM (F). (G–I) Corresponding control for (D to F) where the MIR165/166 biosensor has been rendered insensitive to MIRNA activity. Bars represent 20 μm.

DOI: <https://doi.org/10.7554/eLife.27421.005>

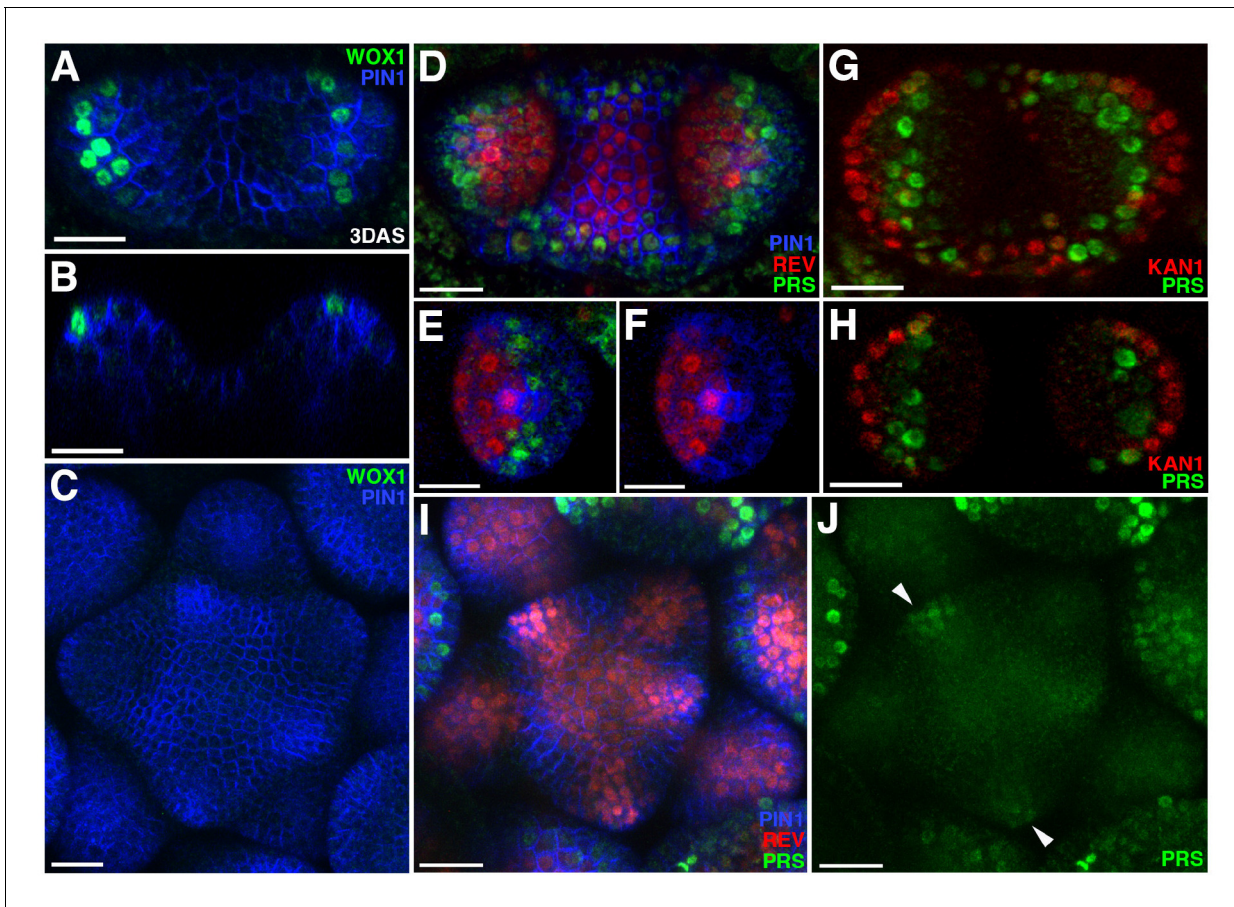


Figure 4. Expression patterns of $2 \times \text{GFP-WOX1}$ and $\text{PRS-2} \times \text{GFP}$. Confocal projections showing PIN1-CFP (blue) and $2 \times \text{GFP-WOX1}$ (green) expression patterns in the vegetative meristem and leaves of seedlings at 3 DAS. (B) Longitudinal section of meristem shown in (A). (C) An inflorescence meristem image showing $2 \times \text{GFP-WOX1}$ is not expressed in the IM. (D) Confocal projection showing PIN1-CFP (blue), $\text{PRS-2} \times \text{GFP}$ (green) and $\text{REV-2} \times \text{YPet}$ (red) expression in the vegetative meristem and leaves at 3.5 DAS, where $\text{PRS-2} \times \text{GFP}$ is expressed surrounding the VM and along the leaf margins. (E and F) Cross sections of leaf on the right side in (D) showing the expression of $\text{PRS-2} \times \text{GFP}$ in the middle domain of the leaf. (G and H) Confocal projection and cross section showing $\text{PRS-2} \times \text{GFP}$ (green) and $\text{KAN1-2} \times \text{CFP}$ (red) expression patterns in the vegetative meristem and leaves of seedlings at 3 DAS. (I and J) $\text{PRS-2} \times \text{GFP}$ (green) is expressed in the young floral bracts in the IM, indicated with arrowhead in (J). Bar = 20 μm .

DOI: <https://doi.org/10.7554/eLife.27421.006>

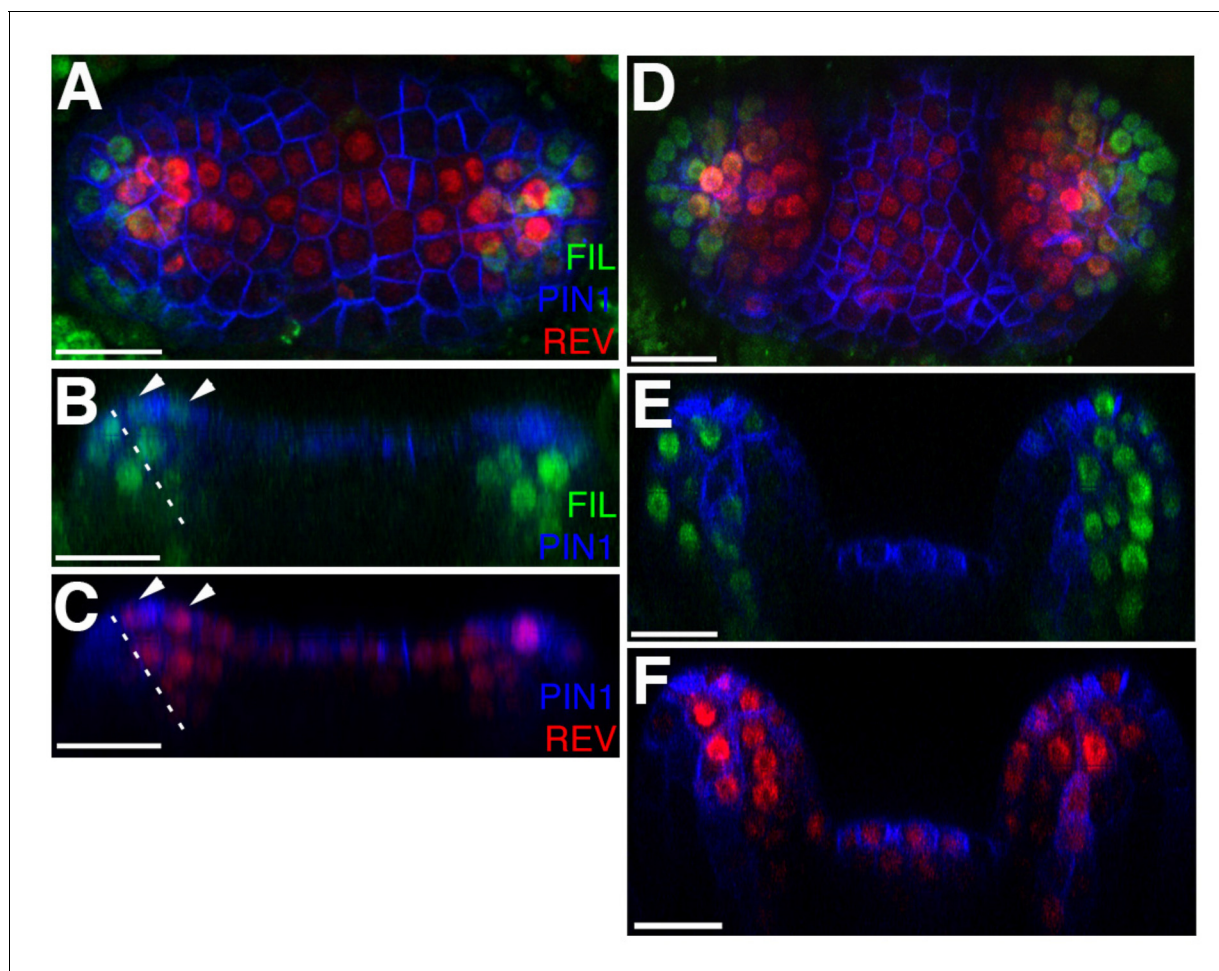


Figure 5. *FILp::dsREDN7* expression is broad during leaf initiation but is later excluded from dorsal tissues. (A–F) Confocal projections and reconstructed sections of seedlings expressing *FILp::dsREDN7* (green), REV-2 \times VENUS (red) and PIN1-CFP (blue). (A) Top view of seedling at 3DAS (B–C) Longitudinal section of seedling shown in (A). Dashed line shows dorsoventral axis of first leaf and arrowheads mark dorsal cells expressing both REV-2 \times VENUS and *FILp::dsREDN7*. (D) Seedlings at 3.5 DAS with *FILp::dsREDN7* expression more restricted to the developing ventral side of the leaf. (E–F) Longitudinal sections of seedling shown in (D) showing a more complementary pattern of *FILp::dsREDN7* relative to REV-2 \times VENUS compared to the earlier stage shown in (A) to (C). Scale bars represent 20 μ m.

DOI: <https://doi.org/10.7554/eLife.27421.007>

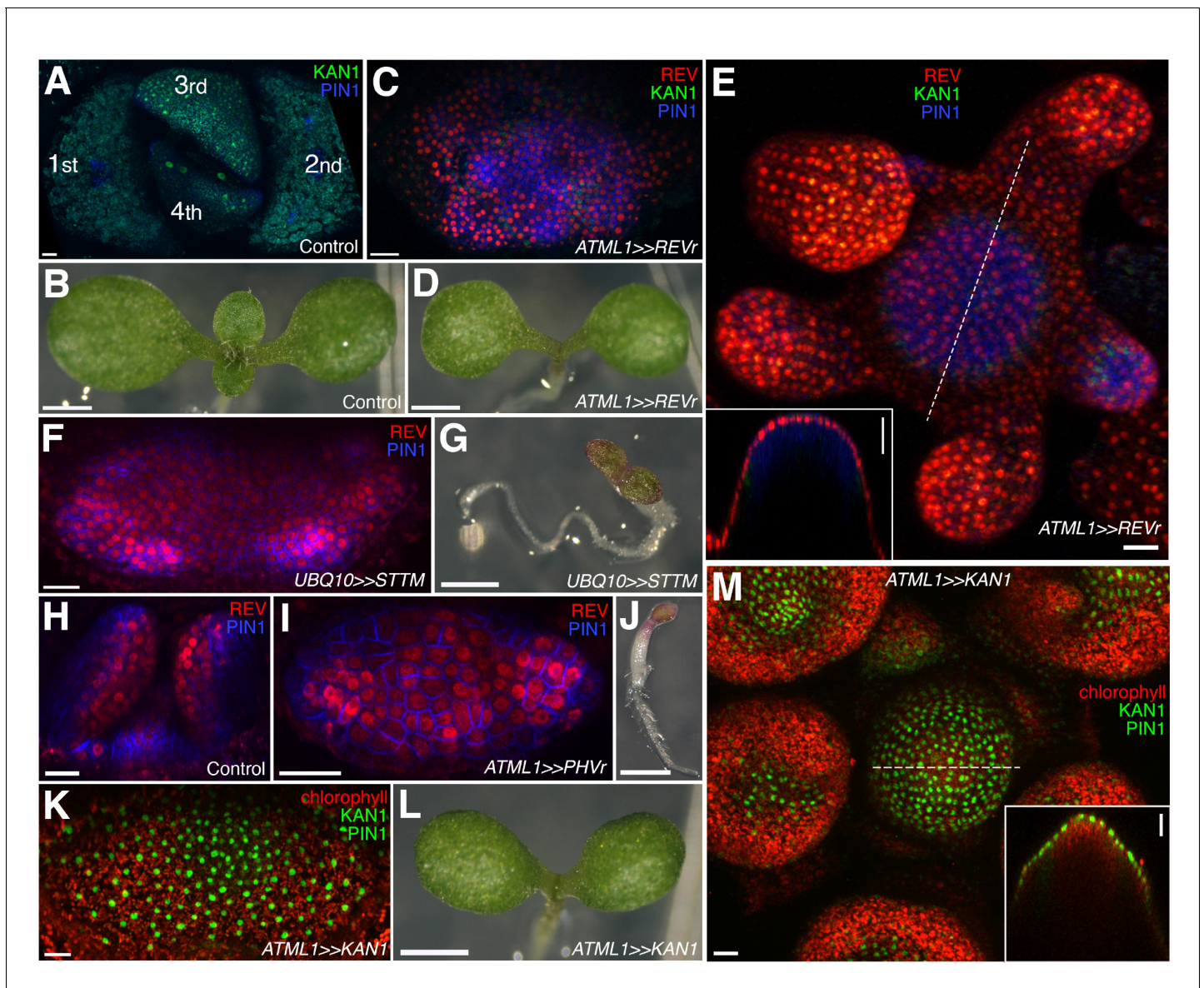


Figure 6. Organ initiation depends on the restriction of Class III HD-ZIP and KANADI expression in the shoot. (A) Confocal projection showing wild type control seedling at 7DAS viewed from above for comparison to (C) and (F). (B) Macroscopic view of control seedling at 7DAS for comparison to (D), (G) and (L). (C) Arrest of organogenesis after ectopic expression of REVr-2 × VENUS from the *ATML1* promoter in the vegetative meristem (7 DAS) after germination on DEX, KAN1-2 × GFP (green) expression is down regulated and could only be detected in a few cells in the sub-epidermis. Although PIN1-CFP (blue) expression is patchy, no leaves developed. (D) Macroscopic view of plant in (C). (E) Arrest of organogenesis after ectopic expression of REVr-2 × VENUS (red) from the *ATML1* in the IM after 3 DEX treatments over 6 days. Note the absence of KAN1-2 × GFP signal. Inset shows longitudinal optical section of the meristem across the dashed line. (F) Seedlings at 7DAS showing similar phenotype to (C) after induction of a short tandem target mimic (STTM) designed to down regulate MIR165/166 activity. (G) Macroscopic view of plant in (F). (H–J) Ectopic expression of REV-2YPet (red) and arrest of organogenesis (PIN1-CFP in blue) in 4DAS seedling after induction of MIR165/166 resistant PHAVOLUTA. (H) Longitudinal view of un-induced control. Top view (I), and macroscopic view (J) of induced seedling showing arrest of organ development. (K and L) Confocal projection (K) and macroscopic view (L) of seedling at 7DAS after induction of KAN1-GFP (green) in the epidermis. No leaves have developed (autofluorescence shown in red). (M) Arrest of organogenesis after induction of KAN1-GFP (green) driven by the *ATML1* promoter in the IM after 3 DEX treatments over 6 days; autofluorescence (red). Inset shows longitudinal optical section of the meristem across the dashed line. Scale bars represent 20 μm in (A, C, E, F, H–I, K and M); 1 mm in (B, D, G, J and L).

DOI: <https://doi.org/10.7554/eLife.27421.008>

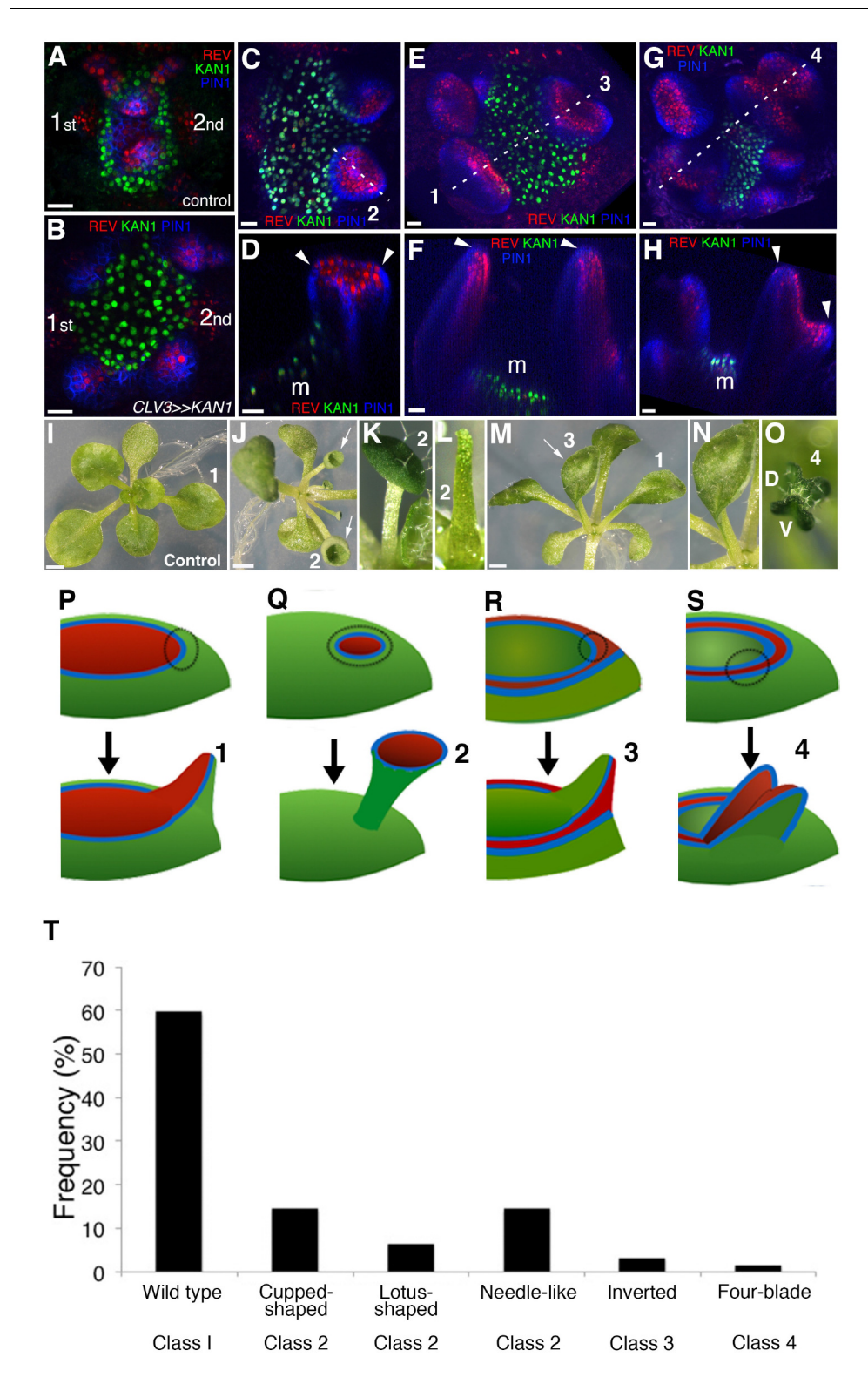


Figure 7. KANADI1 expression boundaries in the shoot specify organ position and orientation. (A and B) Confocal projections showing organ initiation marked by REV-2 × YPet (red) and PIN1-CFP (blue) at border of KAN1-2 × GFP expression (green) in wild type (A) and after induction of KAN1-2 × GFP using the CLV3 promoter (B). Distance separating opposite organs was greater for induced (B) compared to control (A) (Figure 7 continued on next page)

Figure 7 continued

($114.3 \pm 3.3 \mu\text{m}$, $n = 19$ vs $54.2 \pm 1.0 \mu\text{m}$, $n = 10$ (mean \pm SE, $p < 0.05$, t-test)). (C–H) Confocal projections (C, E and G) and longitudinal reconstructions corresponding to dashed lines (D, F and H respectively) showing restricted REV-2 \times YPet expression (red) after ectopic KAN1–2 \times GFP induction (green). Regions in which neither REV-2 \times YPet nor KAN1–2 \times GFP signal was detected may potentially express endogenous KAN1, which was not monitored. Four main configurations of REV expression and morphology were observed (labeled 1 to 4). Class 1 organs (E and F) correspond to the wild type, Class 2 (C and D) express REV-2 \times YPet centrally, Class 3 (E and F) express REV-2 \times YPet in a reversed orientation and Class 4 (G and H) express REV-2 \times YPet centrally and laterally only. Correspondence between REV-2 \times YPet expression boundaries and leaf margins indicated by arrowheads in D, F and H; m indicates meristem. Gamma value changed to highlight PIN1-CFP expression (blue) in (C) to (H). (I–O) Examples of mature leaves corresponding to Classes 1 to 4, including the WT (I), cup-shaped (J), lotus-shaped (a variation of cup-shaped) (K), needle-like (a further decrease in extent of dorsal tissue compare to cup-shaped) (L), inverted (M and N) and four bladed (O). 'D and V' represent 'dorsal' and 'ventral' respectively in (O). (P to S) Diagrams summarizing proposed configurations of REV and KAN (green) gene expression in leaf founder cells (dashed circles) (upper diagram) leading to the observed phenotypic classes of leaf shape (numbered 1 to 4) (lower diagram) after induction of KAN1–2 \times GFP using the CLV3 promoter. (P) represents the wild type Class 1 configuration, (Q) represents Class 2, (R) represents Class 3 and (S) represents Class 4. (T) Frequency of seedlings exhibiting different leaf morphologies after ectopic induction of KAN1–2 \times GFP expression in the CLV3 domain Class of phenotype corresponds to those indicated in (I to O). Scale bars = $20 \mu\text{m}$ in A to H; 1 mm in I, J and M.

DOI: <https://doi.org/10.7554/eLife.27421.009>

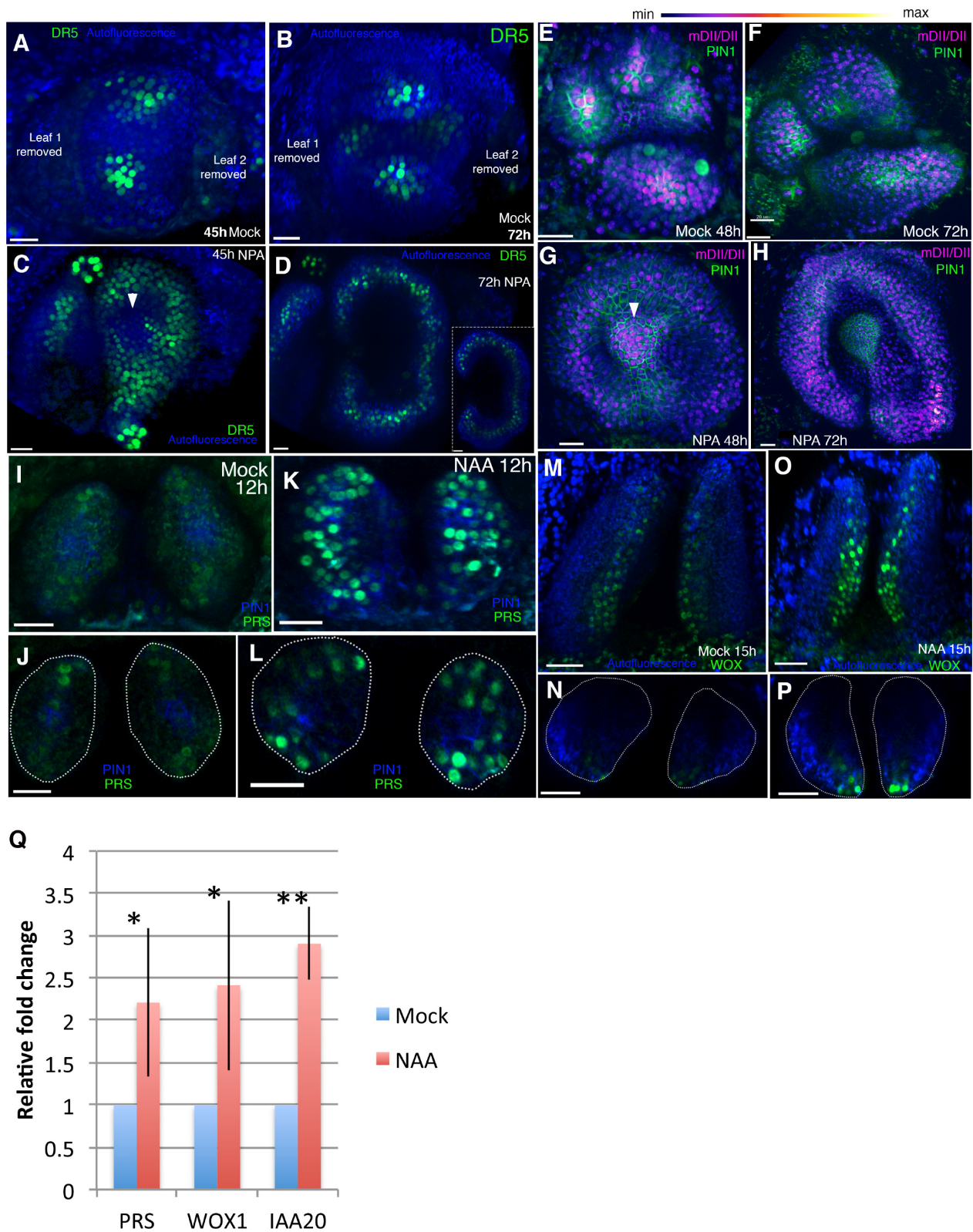


Figure 8. Auxin promotes PRS and WOX expression. (A–D) Response of pDR5V2–3 × VENUS-N7 (green) auxin transcriptional reporter to NPA in Arabidopsis seedlings treated at 3DAS (Days after Stratification). (A and B) Confocal projections 45 hr (A) and 72 hr (B) after treatment with mock

Figure 8 continued on next page

Figure 8 continued

solution. **(C and D)** Confocal projections 45 hr **(C)** and 72 hr **(D)** after treatment with 100 μ M NPA solution ($n = 5/5$). White arrowhead in **(C)** marks absence of DR5 reporter in the center of the meristem. Inset in **(D)** shows transverse optical section through the ring-shaped organ showing most DR5 expression localized in the center of the organ. **(E–H)** Expression and response of R2D2 (magenta) to auxin along with PIN1-GFP expression (green) in Arabidopsis seedlings treated at 3DAS. **(E and F)** Confocal projections 48 hr **(E)** and 72 hr **(F)** after treatment with mock solution. **(G and H)** Confocal projections 48 hr **(G)** and 72 hr **(H)** after treatment with 100 μ M NPA solution ($n = 4/4$). White arrowhead in **(G)** marks the presence of auxin in the meristem center (compare with **(C)** which shows absence of auxin signaling in the meristem center). **(I–L)** Expression and response of pPRS::PRS-2 \times GFP to auxin in Arabidopsis seedlings. Confocal projections and transverse optical slices of seedlings 4DAS showing of pPRS::PRS-2 \times GFP expression (green) 12 hr after treatment with mock solution **(I and J)** and 5 mM NAA **(K and L)** ($n = 5/5$). **(M–P)** Expression and response of 2 \times GFP WOX to auxin in Arabidopsis seedlings. **(M and N)** Confocal projections **(M and O)** and corresponding optical slices **(N and P)** of seedlings 4DAS showing pWOX1::2 \times GFP-WOX1 expression (green) 12 hr after treatment with mock solution **(M and N)** and 5 mM NAA **(O and P)**. Note WOX expression increases but does not expand beyond its regular expression domain upon auxin addition ($n = 5/5$). **(Q)** Q-PCR analysis of PRS, WOX1 and positive control IAA20 transcripts after 5 mM NAA or mock treatment on 4 days old wild-type (Ler) seedlings. *= $p < 0.05$, **= $p < 0.001$. Scale bars 20 μ m **(A–I, K)**; 15 μ m **(J and L)**; 30 μ m **(M–P)**.

DOI: <https://doi.org/10.7554/eLife.27421.011>

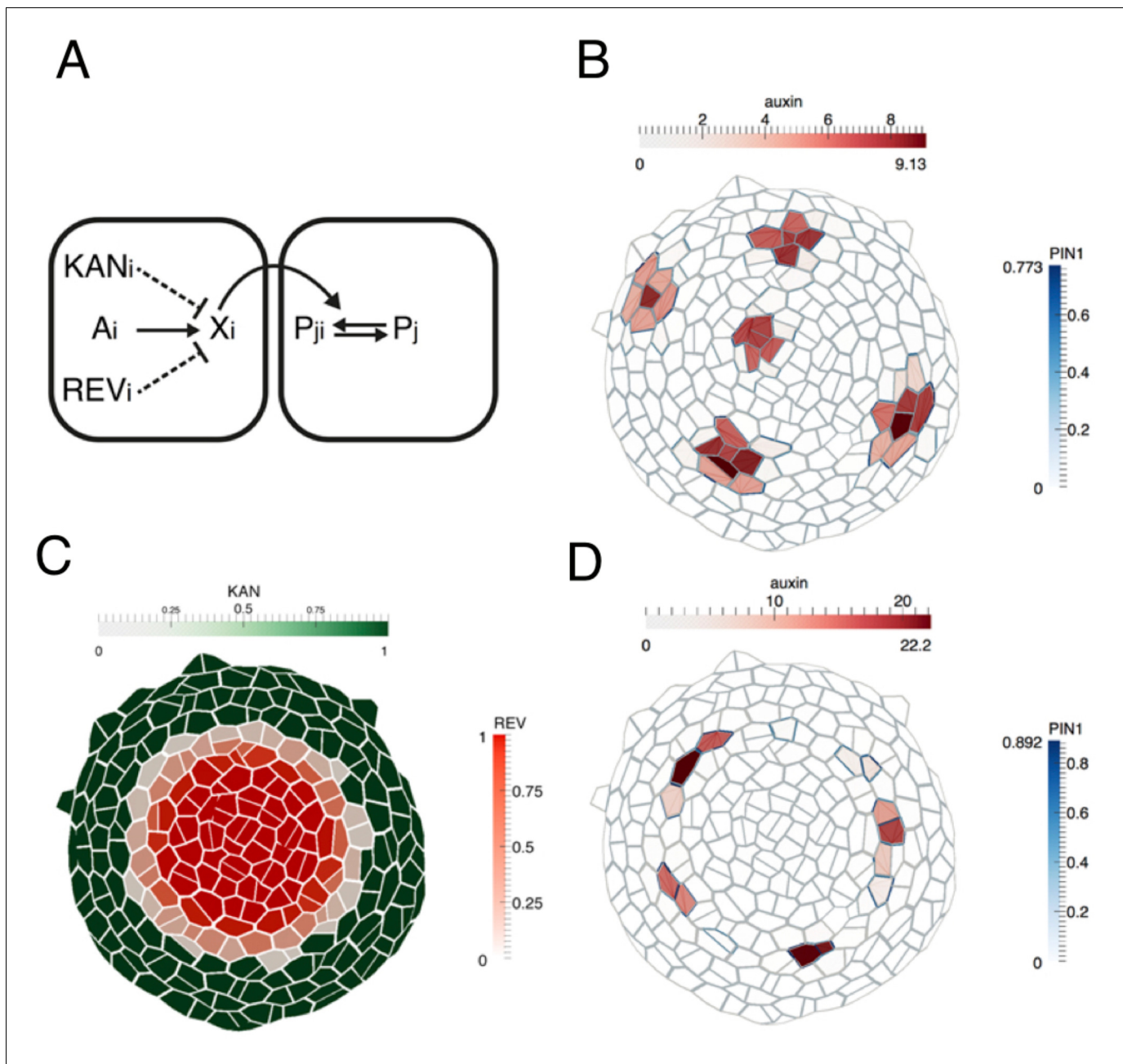


Figure 9. Computational model illustrating how dorsoventral gene expression boundaries may restrict phyllotactic patterning to the SAM peripheral zone. (A) Illustration of model interactions. Auxin is transported passively and actively via PIN1 between cells. PIN1 is polarized towards cells with high auxin, via a signaling pathway represented by X (previously suggested to be realized by increased stresses in the neighboring cells due to changes in mechanical wall properties (Heisler et al., 2010)). (B) As shown previously (Heisler et al., 2010; Jönsson et al., 2006; Smith et al., 2006), peaks of auxin are formed spontaneously. (C) A pattern of KANADI (green) and REVOLUTA (red) is added to the template with a boundary domain in between in which REV expression is low or absent and KAN1 expression is absent. (D) If KANADI and REVOLUTA decrease the signal X in cells where they are expressed (dashed interactions in A), the formation of auxin peaks is restricted to the boundary.

DOI: <https://doi.org/10.7554/eLife.27421.013>

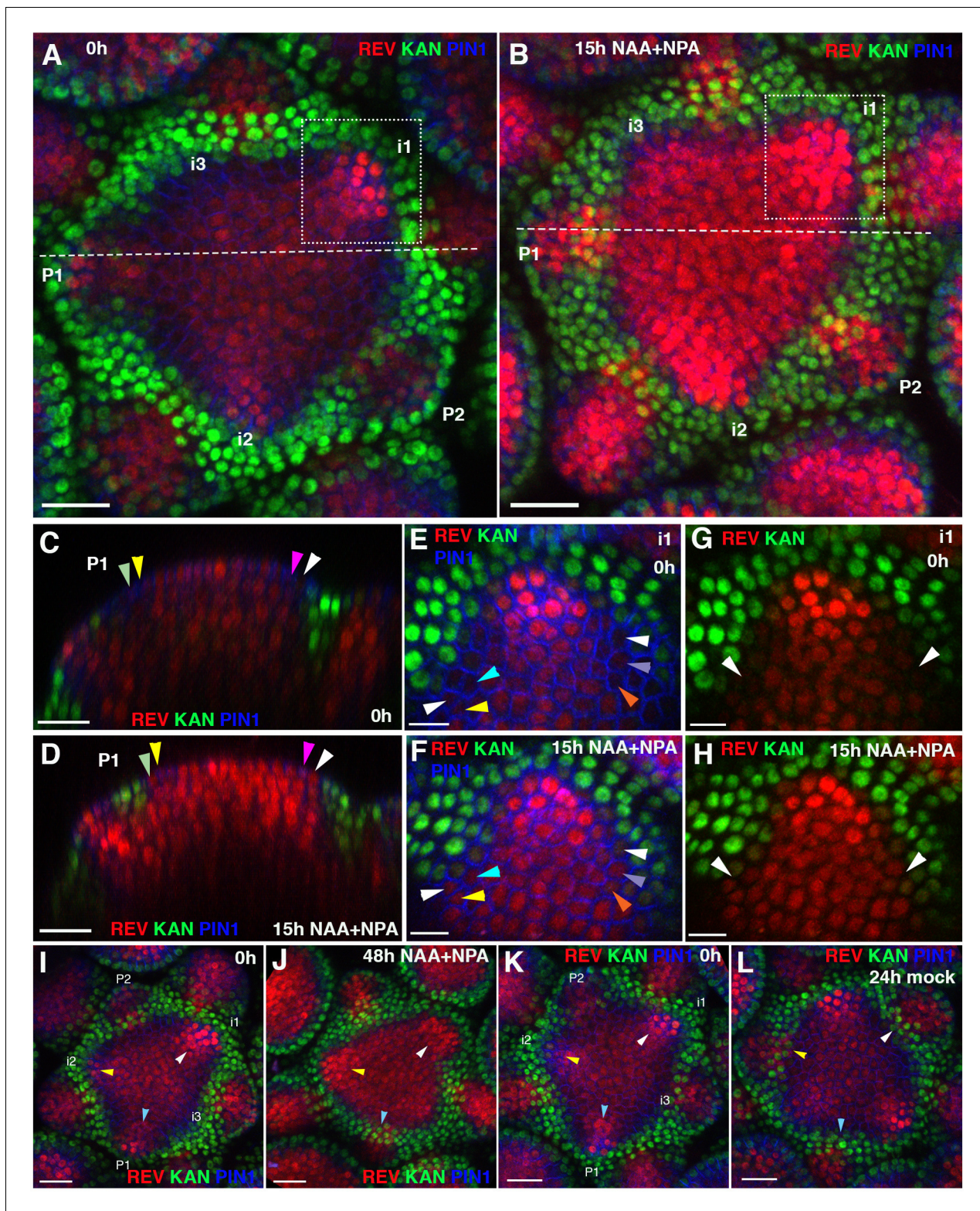


Figure 10. Effect of auxin on the expression patterns of REV and KAN1 in the inflorescence meristem. (A and B) Confocal projections of the IMs showing expression pattern of REV-2 × YPet (red), KAN1-2 × GFP (green) and PIN1-CFP (blue) before (A) and 15 hr after the combined application of 5 mM NAA and 100 μM NPA (B). Primordium (P) and incipient primordium (i) stages are numbered from i3-P2 based on convention described in (Heisler et al., 2005). Note up regulation and expansion of REV expression 15 hr after the combined application of NAA and NPA (n = 6). (C and D) Longitudinal optical sections along the dashed white lines in (A) and (B) respectively. Note the presence of REV expression in the epidermal cells

Figure 10 continued on next page

Figure 10 continued

marked by arrowheads in (D) and a corresponding absence or weak level of expression in (C). Similar colored arrowheads mark the same cells tracked over 15 hr. (E and F) Magnified views of the surface of i1, outlined by dotted rectangles in (A and B) showing expression pattern of REV-2 ×YPet (red), KAN1–2 × GFP (green) and PIN1-CFP (blue) before (E) and 15 hr after the combined application of 5 mM NAA and 100 μM NPA (F). Note the presence of REV in the cells marked by arrowheads in (F) and their absence in (E). Similar colored arrowheads mark the same cells tracked over 15 hr in (E and F). (G and H) Same as (E and F) but showing REV and KAN1 expression only. Note the presence of a gap between REV and KAN1 expression in (G) but its absence in (H), marked by white arrowheads in (G and H). (I–L) Confocal projections of IMs showing expression of REV-2 ×YPet (red), KAN1–2 × GFP (green) and PIN1-CFP (blue) before (I) and 48 hr after the combined application of 5 mM NAA and 100 μM NPA (J), and before (K) and 24 hr after treatment with mock solution (L). Initially for both control and treated meristems, KAN1 expression is absent between the meristem center and P1 (blue arrowheads), i1 (white arrowheads) and i2 (yellow arrowheads) (I and K). Under mock treatment, KAN1 expression appears in all three corresponding regions (marked by the same arrowheads) 24 hr later (L). However for the meristem treated with NAA and NPA, KAN1 expression is absent in regions previously corresponding to i1 (white arrowheads) and i2 (yellow arrowheads) but not P1 (blue arrowheads), even after 48 hr (J). Scale bars 20 μm (A–D, I–L) and 10 μm (E–H).

DOI: <https://doi.org/10.7554/eLife.27421.014>

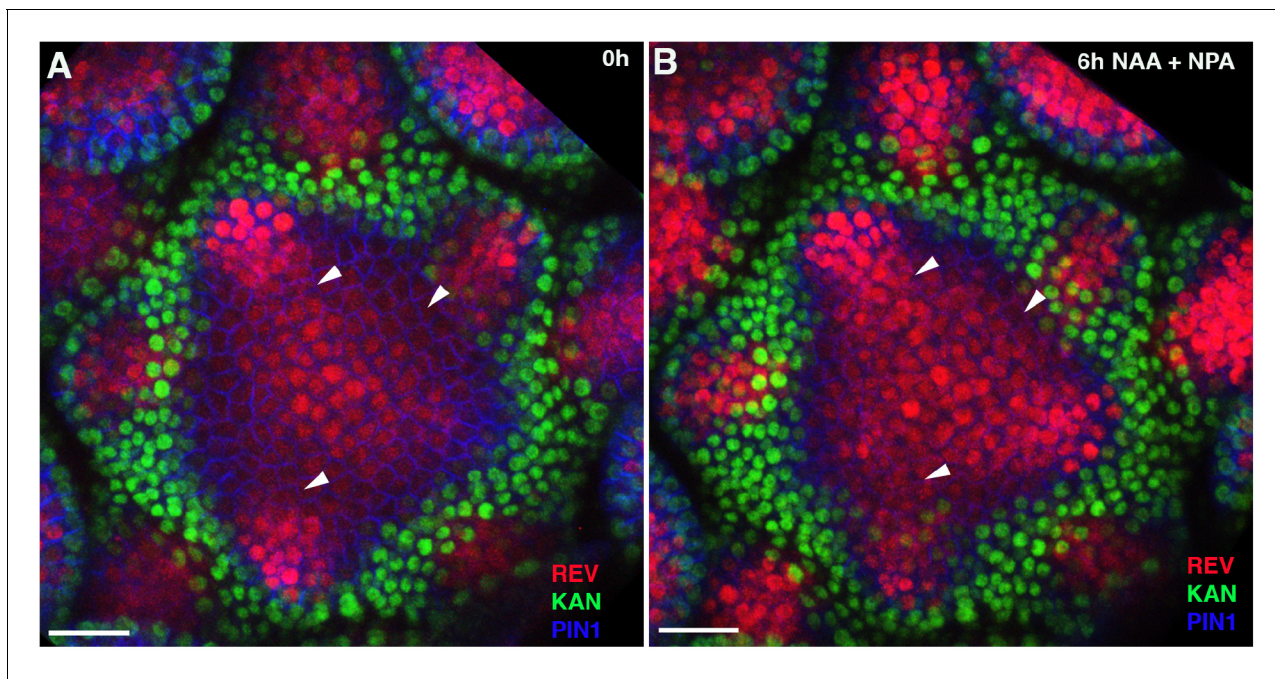


Figure 10—figure supplement 1. REV expression starts to expand within 6 hr of auxin treatment. (A and B) Confocal projections of the IMs showing expression pattern of REV-2 × YPet (red), KAN1-2 × GFP (green) and PIN1-CFP (blue) before (A) and 6 hr after the combined application of 5 mM NAA and 100 μM NPA (B). Note a slight increase and expansion in REV expansion at positions marked by white arrowheads in (B) compared to (A) (n = 4). Scale bars 20 μm (A and B).

DOI: <https://doi.org/10.7554/eLife.27421.015>

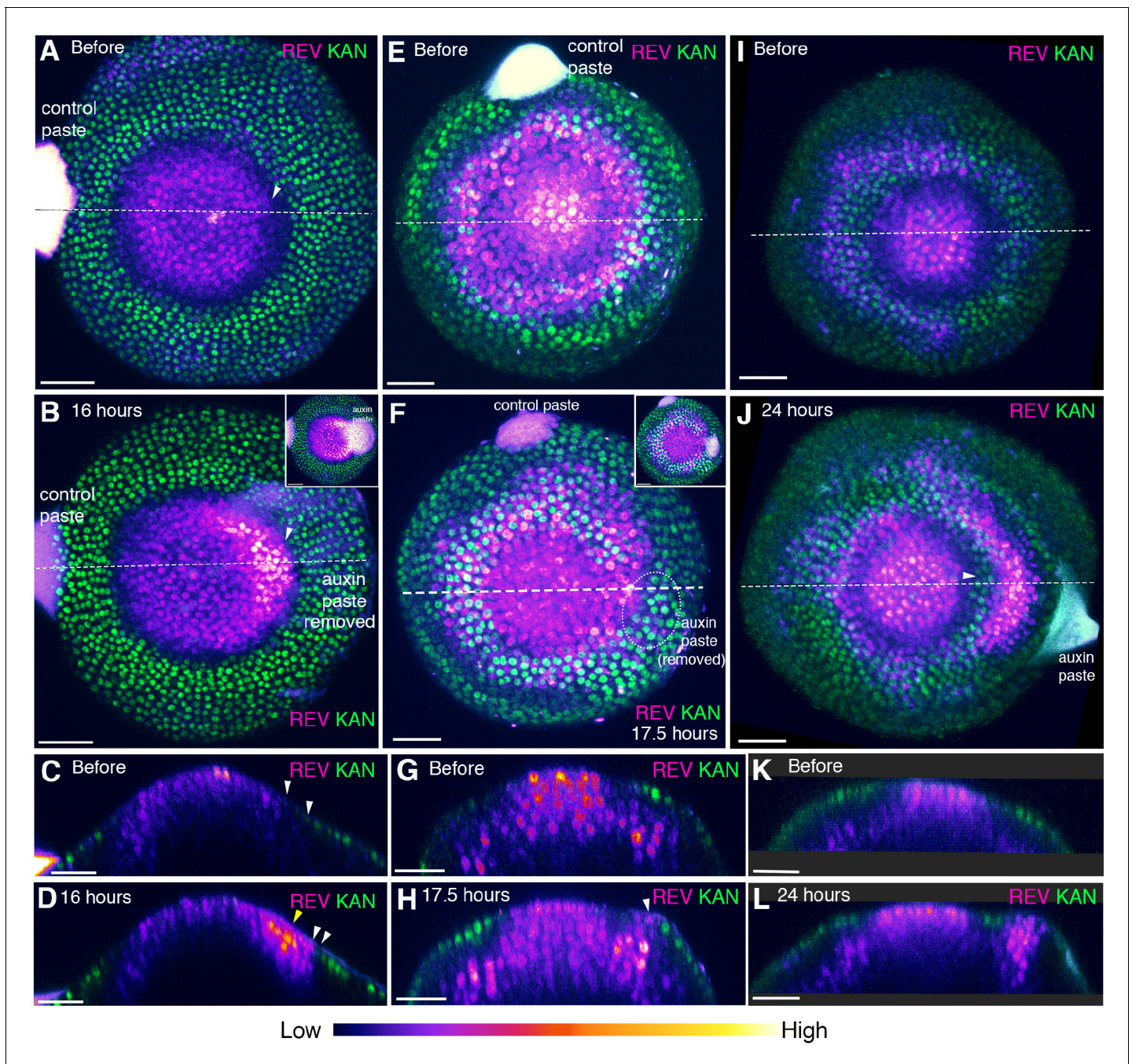


Figure 10—figure supplement 2. Auxin modulates the expression of REV and KAN1 locally. (A–L) Three examples of *pin1-4* mutant meristems showing changes in REV-2 × VENUS (magenta) and KAN1-2 × GFP (green) expression in response to local auxin application (arranged according to developmental stage). (A and B) Confocal projections of *pin1-4* meristem showing pattern before (A) and 16 hr after local auxin application (B). We have used an intensity color code to better show local differences in REV-2 × VENUS expression levels. Note local up-regulation and extension of REV at the site of auxin paste application (white arrowhead, paste was removed to visualize the expression pattern at the site of application). Inset in (B) shows view from above prior to removal of paste. (C and D) Longitudinal optical sections along the dashed white lines in (A) and (B) respectively. Note strong up regulation of REV at the site of auxin paste application (yellow arrowhead in (D)) and the presence of a gap between REV and KAN1 expression (white arrowheads) prior to local auxin application (C) and reduction in this gap due to REV expansion in (D) ($n = 5/6$). (E and F) Confocal projections showing pattern before (E) and 17.5 hr after local auxin application (F). Inset in (F) shows view prior to removal of paste. (G and H) Longitudinal optical sections along the dashed white lines in (E) and (F) respectively. Note the extension of REV into the developing primordium (white arrowhead in (H)). (I and J) Confocal projections showing pattern before (I) and 24 hr after local auxin application (J). Note the local pattern of both REV and KAN1 expression induced at the site of auxin application (white arrowhead in (J)). (K and L) Longitudinal optical sections along the dashed white

Figure 10—figure supplement 2 continued

lines in (I) and (J) respectively. Note REV expression in the center of the organ primordium surrounded by KAN expression on both the sides (L) (n = 3). Scale bars 40 μm (A and B), 30 μm (C and D, E–L).

DOI: <https://doi.org/10.7554/eLife.27421.016>

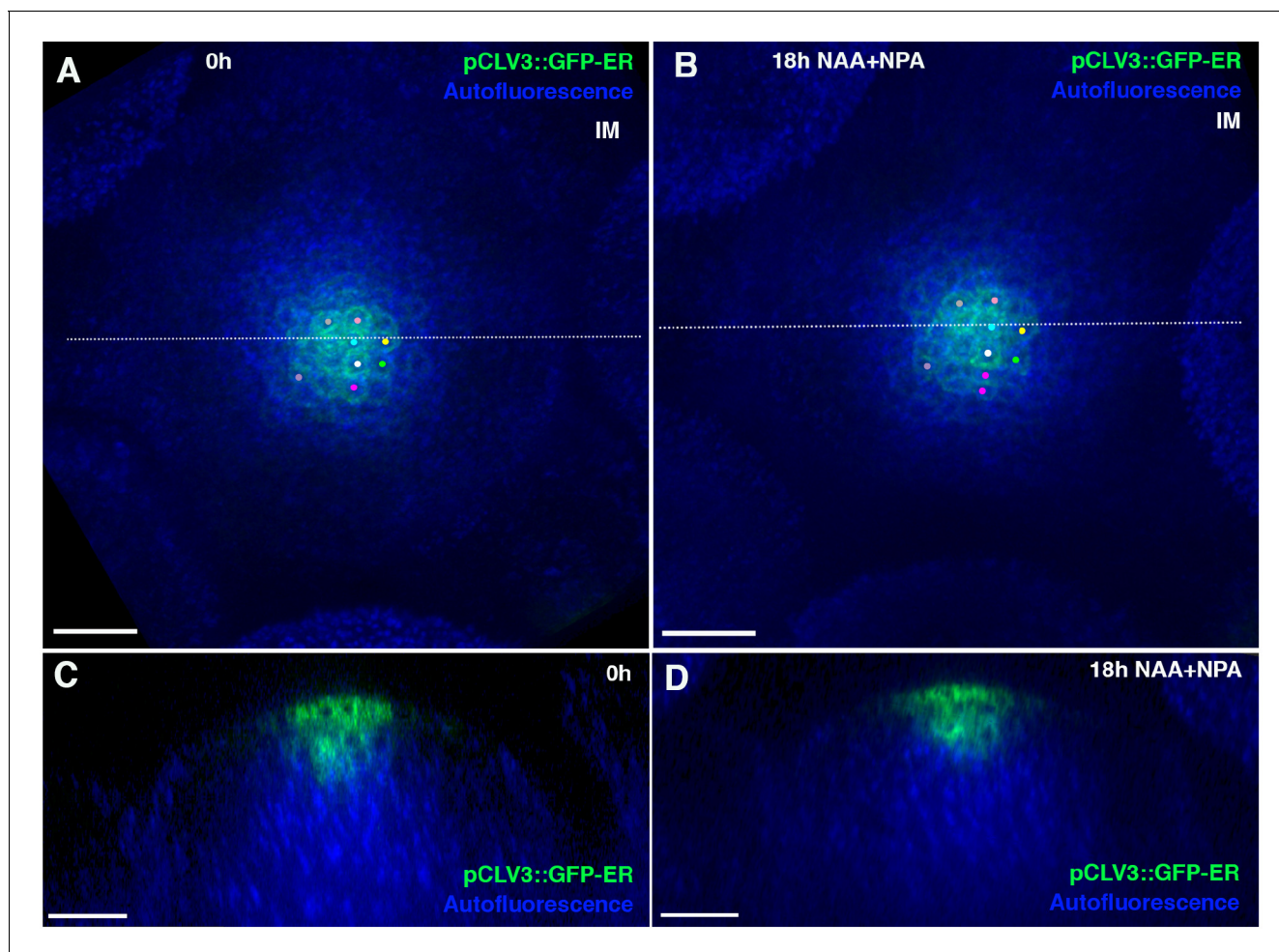


Figure 10—figure supplement 3. Auxin application does not expand CLAVATA3 expression and hence, the central zone of the meristem. (A and B) Confocal projections of IM showing expression of pCLAVATA3::GFP-ER (green) before (A) and 18 hr after combined application of NAA and NPA. Cells expressing GFP-ER have been tracked using similar colored dots over 18 hr (A and B). (C and D) Longitudinal optical sections along the dashed white lines in (A) and (B) respectively. Note no significant expansion in CLAVATA3 expression (B and D) 18 hr after auxin application (n = 4). Scale bars 20 μm (A–D).

DOI: <https://doi.org/10.7554/eLife.27421.017>

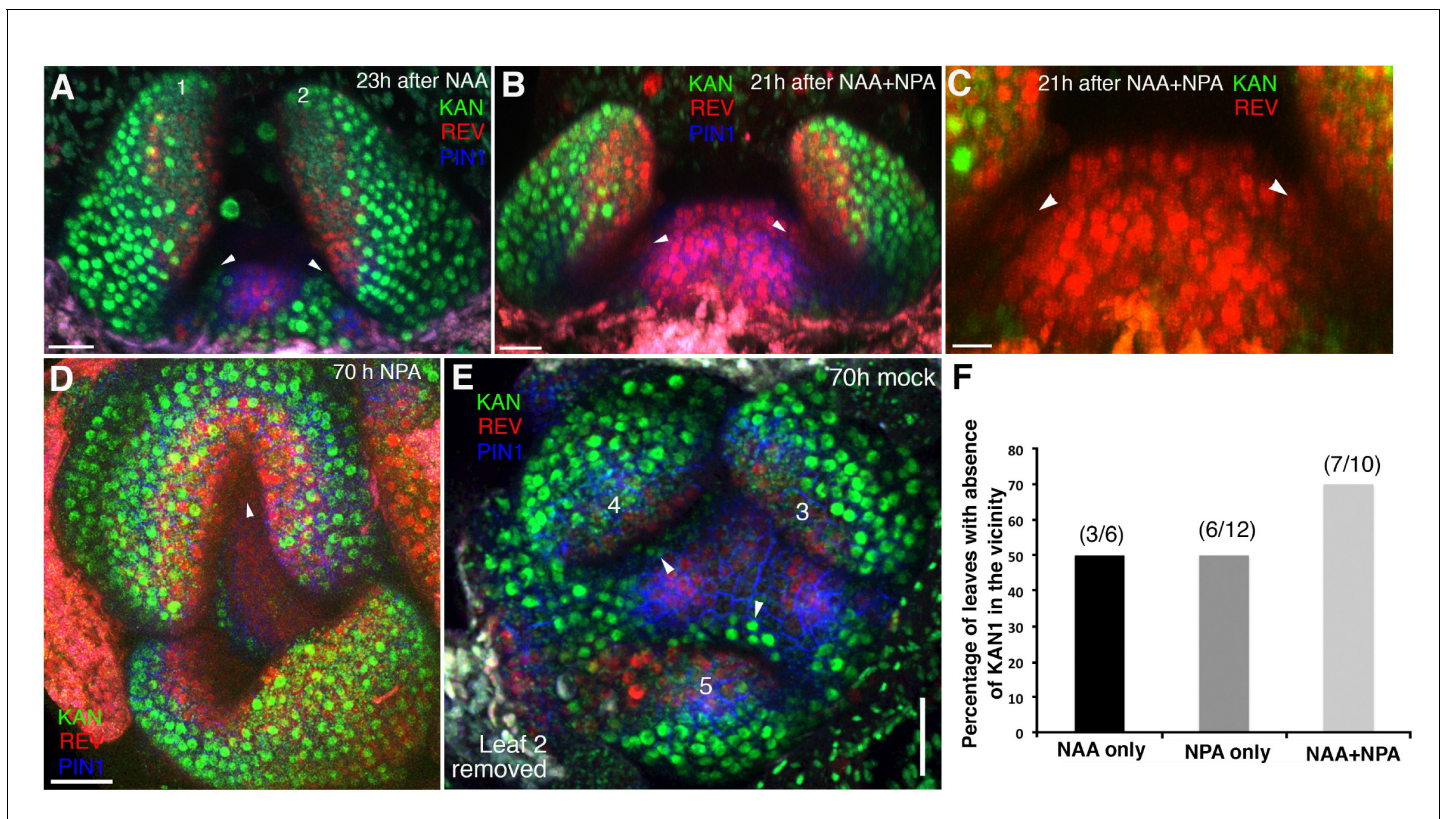


Figure 11. High auxin levels prevent new KAN1 expression in the leaf axils. (A–E) Confocal projection of the VM showing expression pattern of REV-2 × YPet (red), KAN1-2 × GFP (green) and PIN1-CFP (blue) 23 hr after the treatment with 5 mM NAA (A), 21 hr after combined treatment with NAA and NPA (B and C); panel (C) showing close-up view of the meristem in (B) with REV (red) and KAN1 (green) expression only, 70 hr after treatment with NPA alone (D) and 70 hr after treatment with mock (E). White arrowheads mark the presence of KAN1 expression in the cells adjacent to the grown out leaves in (A) and (E) and absence in (B–D). Note that REV expression (red) expanded towards leaves axils in (B–D). However also note that REV expression appears faint in the leaf axils in (B and C) compared to (D). This is due to the reason that the combined application of NAA and NPA resulted in the leaves growing at an acute angle to the meristem, which caused shading and made it difficult to reach leaf axils while imaging. (F) A bar graph showing percentages of leaves lacking KAN1 expression in their vicinity upon treatment with NAA, NPA and NAA + NPA. Scale bars 20 μ m (A and B), 10 μ m in (C) and 30 μ m (D and E).

DOI: <https://doi.org/10.7554/eLife.27421.018>

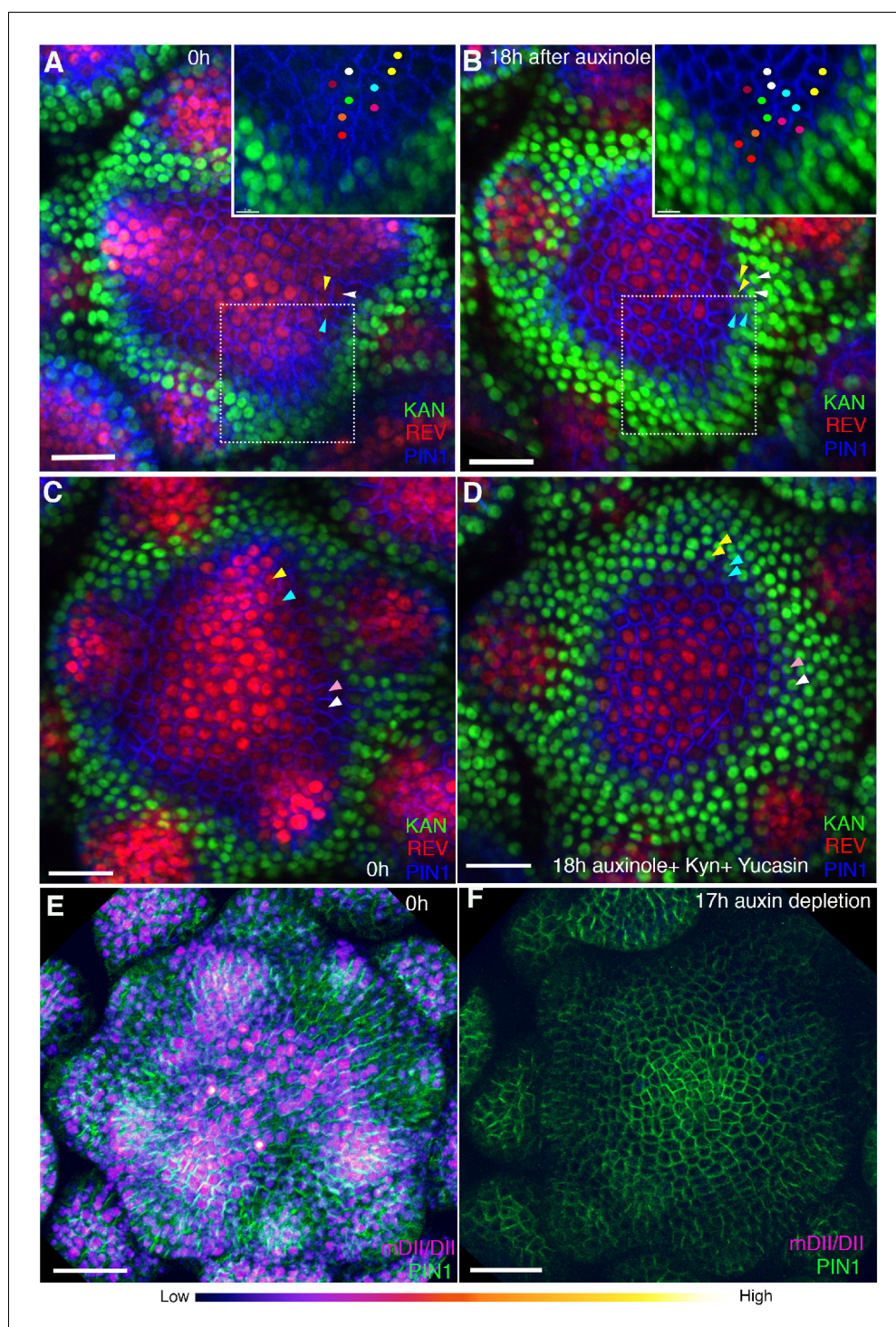


Figure 12. Auxin depletion alters boundary position. (A and B) Confocal projections of the IMs showing expression pattern of REV-2 × YPet (red), KAN1–2 × GFP (green) and PIN1-CFP (blue) before (A) and 18 hr (B) after the application of 100 μM auxinole. Inset shows close-up of the primordium outlined with the dotted rectangle. Similar colored dots mark the same cells at 0 hr and 18 hr time-points. Note the presence of KAN1 expression in the proximity of the cells marked with colored dots in the inset in (A) and its absence in the inset in (B). Similar color arrowheads in (A and B) mark the same cells that showed REV expression at 0 hr but KAN1 expression at 18 hr after treatment with auxinole. (C and D) Confocal projections of the IMs showing expression pattern of REV-2 × YPet (red), KAN1–2 × GFP (green) and PIN1-CFP (blue) before (C) and 18 hr (D) after the combined application of 100 μM auxinole, 100 μM KYN and 100 μM Yucasin (auxin depleting drugs). Note KAN-
Figure 12 continued on next page

Figure 12 continued

2 ×GFP expression has expanded centrally at the expense of REV-2 × YPet expression (compare the cells marked by arrowheads in (C) with (D), similar colored arrowheads mark the same cells tracked over 18 hr) ($n = 6/6$). (E and F) Confocal projections of the IMs indicating the predicted auxin distribution (magenta) based on R2D2 expression along with PIN1-GFP expression (green) before (E) and 17 hr after the combined application of 100 μ M auxinole, 100 μ M kyn and 100 μ M yucasin (auxin depleting drugs) (F). Note lack of detectable auxin based on R2D2 expression in (F) compared to (E) after the combined drug application ($n = 3/4$). Scale bars 20 μ m (A–D), 30 μ m (E and F).

DOI: <https://doi.org/10.7554/eLife.27421.020>

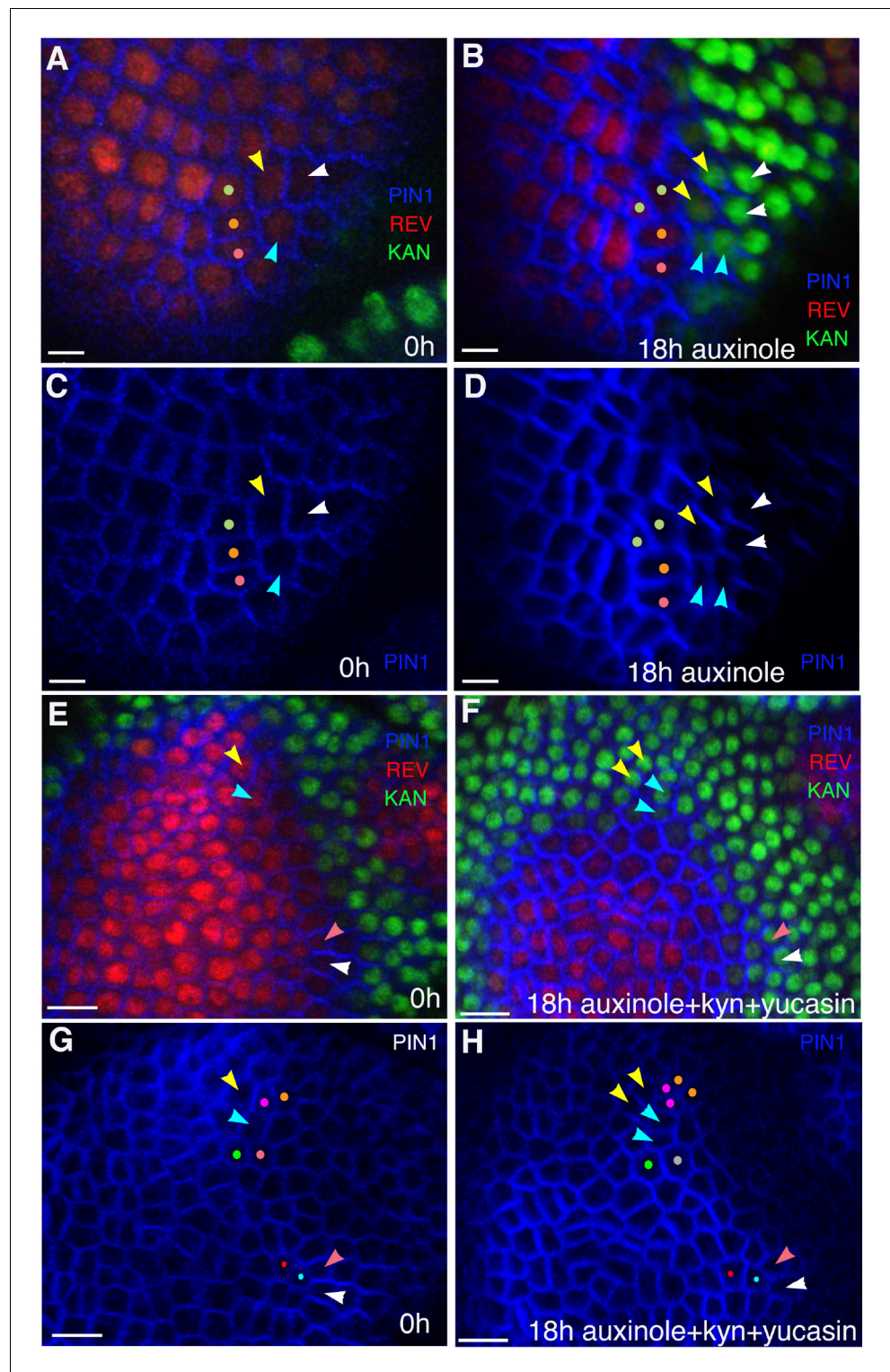


Figure 12—figure supplement 1. Auxin depletion results in KAN expression at the expense of REV. (A and B) Close-up views of cells marked with arrowheads in **Figure 12A** (A) and **Figure 12B** (B) showing PIN1 (blue), KAN (green) and REV expression (red). Similar colored arrowheads mark the same cells tracked over 18 hr (same as in **Figure 12** (A and B)). (C and D) Same as (A and B) but showing PIN1 expression alone to clearly highlight cell outlines for their identification after 18 hr of treatment with auxinole. (E and F) Close-up views of the cells marked with arrowheads in **Figure 12C** (E) and **Figure 12D** (F) showing PIN1 (blue), KAN (green) and REV expression (red). *Figure 12—figure supplement 1 continued on next page*

Figure 12—figure supplement 1 continued

Similar colored arrowheads mark the same cells tracked over 18 hr (same as in **Figure 12 (C and D)**). (**G and H**) Same as (**E and F**) but showing PIN1 expression alone to clearly highlight cell outlines for their identification, 18 hr after combined treatment with auxinole, yucasin and kyn. Cells marked with same colored dots are tracked over 18 hr in (**A–H**). Scale bars, 5 μm (**A–D**) and 10 μm (**E–H**).

DOI: <https://doi.org/10.7554/eLife.27421.021>

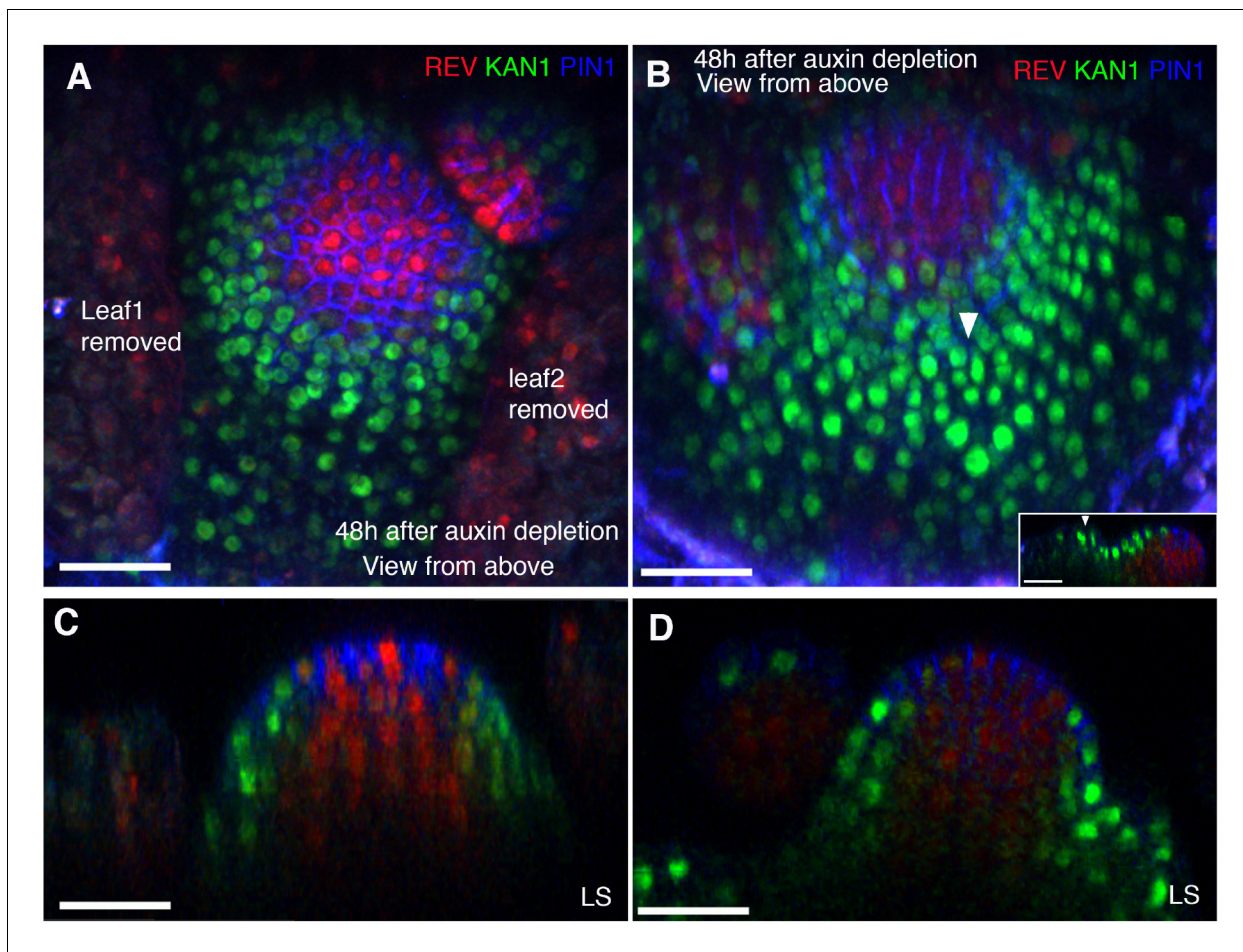


Figure 12—figure supplement 2. Auxin depletion alters dorsoventral gene expression in the vegetative meristems. (A and B) Confocal projections of the VMs showing expression pattern of REV-2 × YPet (red), KAN1-2 × GFP (green) and PIN1-CFP (blue) 48 hr after the combined application of 100 μ M auxinole, 100 μ M KYN and 100 μ M Yucasin (auxin depleting drugs). Arrowhead in (B) marks an arrested leaf primordium expressing KAN throughout. Inset in (B) shows a longitudinal optical section of the leaf primordium ectopically expressing KAN1-2 × GFP. (C and D) Longitudinal optical sections of the VMs in (A) and (B) respectively. Note that the meristems grow as pins with no new organs initiating. Scale bars 30 μ m (A-D, inset in B).

DOI: <https://doi.org/10.7554/eLife.27421.022>

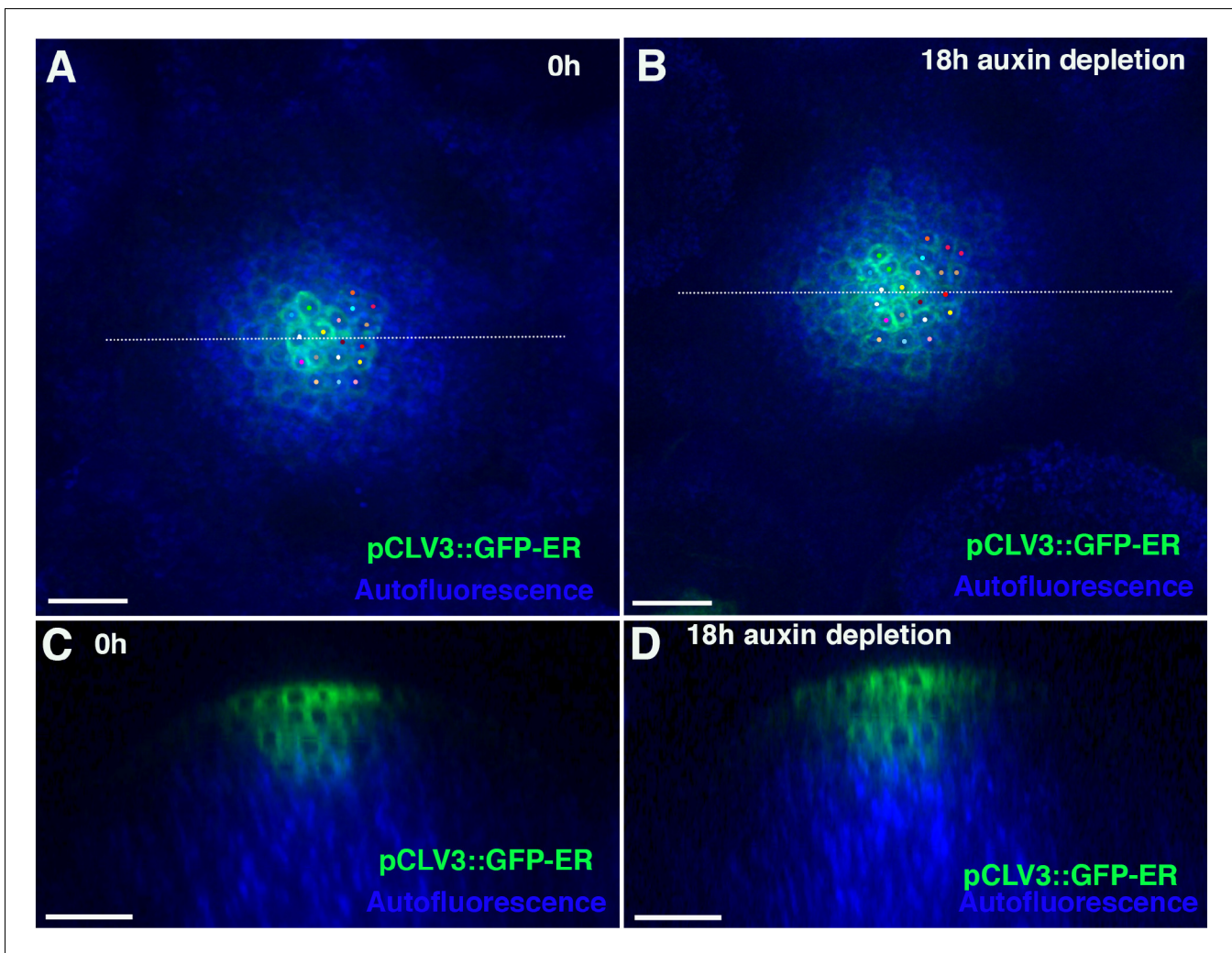


Figure 12—figure supplement 3. Auxin depletion does not results in the shrinking of the central zone of the meristem. (A and B) Confocal projections of the IMs showing expression of pCLAVATA3::GFP-ER (green) before (A) and 18 hr after combined application of auxin depleting drugs. Cells expressing GFP-ER have been tracked using similar colored dots over 18 hr (A and B). (C and D) Longitudinal optical sections along the dashed white lines in (A) and (B) respectively. Note no significant reduction in the zone of CLAVATA3 expression (B and D) 18 hr after auxin depletion. Scale bars 20 μm (A–D) (n = 4).

DOI: <https://doi.org/10.7554/eLife.27421.023>

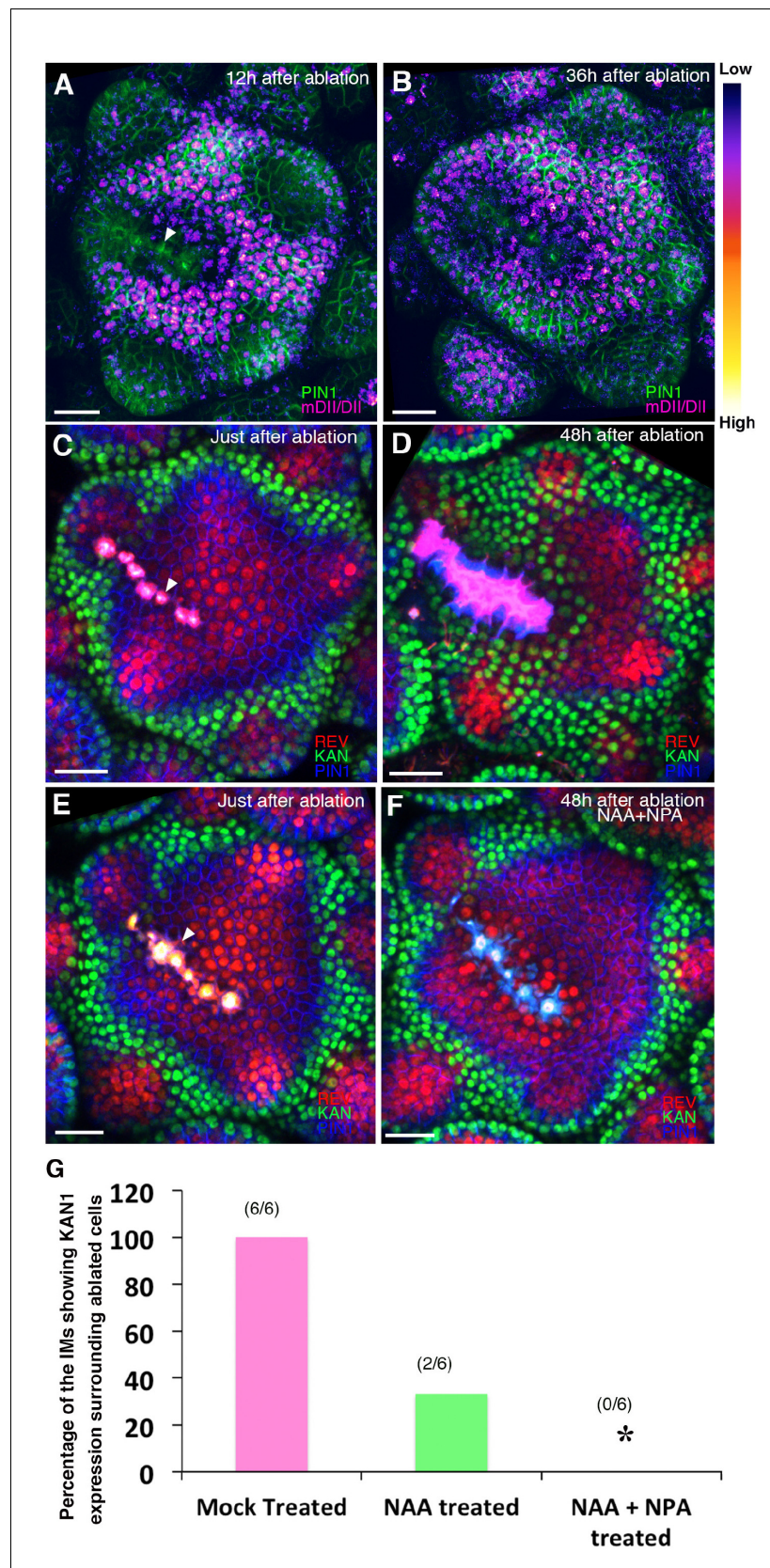


Figure 13. Wounding induces KANADI1 expression in response to low auxin. (A and B) Confocal projections of IMs showing predicted auxin distribution (magenta) based on R2D2 expression 12 hr (A) and 36 hr (B) after

Figure 13 continued on next page

Figure 13 continued

wounding. Note low predicted auxin levels in the cells surrounding the ablated cells. **(C and D)** Confocal projections of the IMs showing expression pattern of REV-2 \times YPet (red), KAN1–2 \times GFP (green) and PIN1-CFP (blue) immediately after ablation (ablated cells indicated a white arrowhead) **(C)** and 48 hr after **(D)**. Note KAN1 expression (green) has completely surrounded the wounded cells 48 hr after the ablation **(D)** compared to **(C)**. **(E and F)** Confocal projections of the IMs showing expression pattern of REV-2 \times YPet (red), KAN1–2 \times GFP (green) and PIN1-CFP (blue) immediately after ablation (ablated cells are marked by white arrowhead) **(E)** and 48 hr after ablation and combined NAA and NPA application **(F)**. Note absence of KAN1 expression (green) surrounding the wound when wounding is accompanied by the exogenous addition of auxin and NPA (compare to **(D)**). **(G)** Quantification of wounding induced ectopic KAN1 expression upon mock treatment ($n = 6/6$), NAA application ($n = 2/6$) and NAA + NPA combination ($n = 0/6$) application on the Arabidopsis IMs expressing REV-2 \times YPet, KAN1–2 \times GFP and PIN1-CFP. Scale bars 30 μm **(A–F)**.

DOI: <https://doi.org/10.7554/eLife.27421.024>

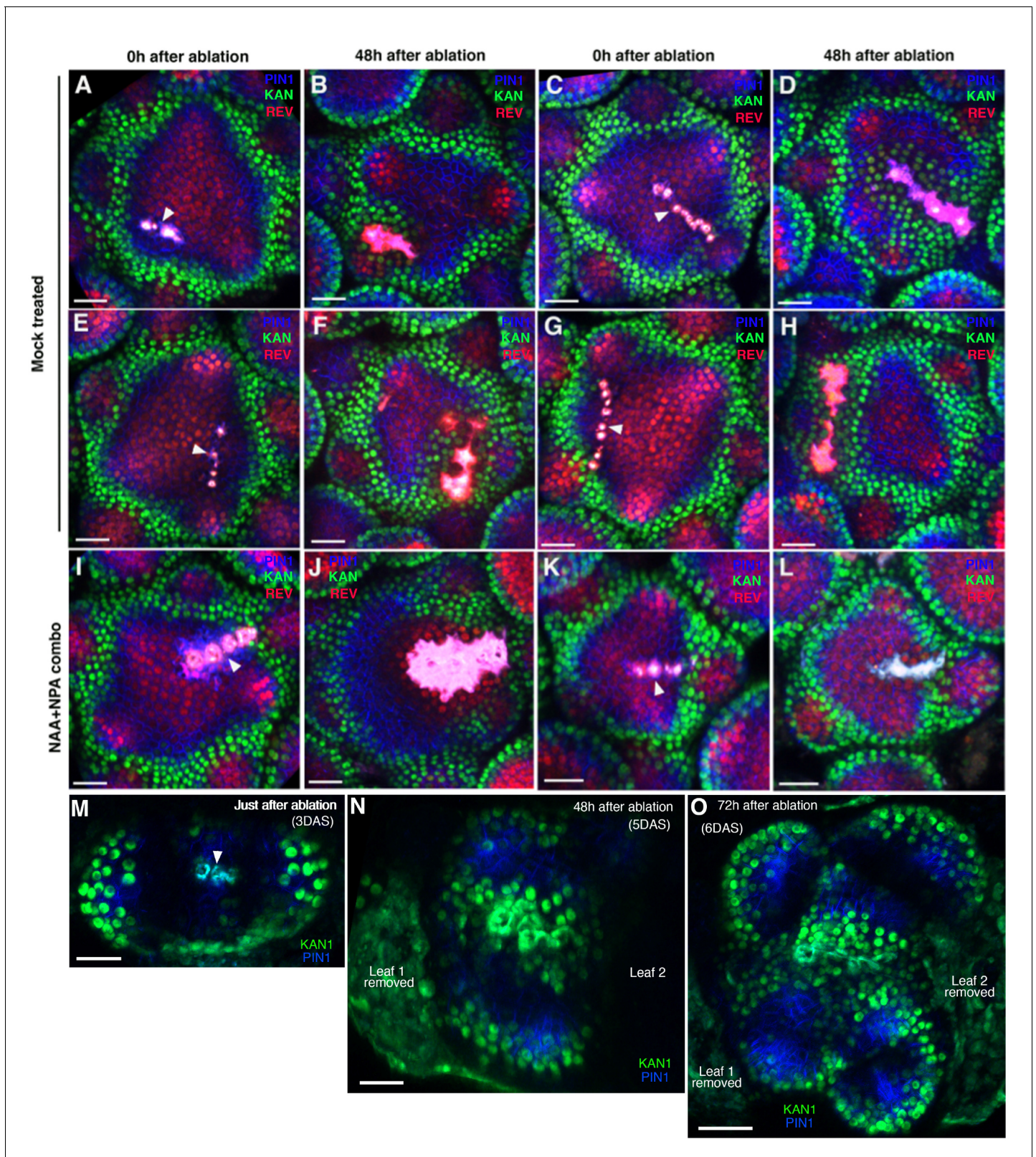


Figure 13—figure supplement 1. Wounding induces ectopic KAN expression in the inflorescence and vegetative meristems. (A–H) Confocal projections of the inflorescence meristems showing expression pattern of KAN1-2 \times GFP (green) and PIN1-CFP (blue) immediately after ablation (A, C, E, and G) and corresponding meristems 48 hr after ablation (B, D, F and H). Note ectopic KAN1 expression on both the sides of the ablated cells 48 hr after ablation. Figure 13—figure supplement 1 continued on next page

Figure 13—figure supplement 1 continued

after wounding. (I–L) Confocal projections of inflorescence meristems showing expression pattern of KAN1–2 × GFP (green) and PIN1-CFP (blue) immediately after (I and K) and 48 hr after ablation and treatment with NAA and NPA (J and L). Note lack of ectopic KAN1 expression compared to comparable untreated meristems (B, D, F and H). (M–O) Confocal projections of the vegetative meristems showing expression pattern of KAN1–2 × YPet (green) and PIN1-GFP (blue) immediately after ablation (M), 48 hr after ablation (N) and 72 hr after ablation (O). Ablated cells are marked by arrowhead in (M). 72 hr after wounding the vegetative meristem appears split into at least two distinct meristems with new leaves oriented normally with respect to each meristem (O). Scale bars 20 μ m (A–N); 30 μ m (O).

DOI: <https://doi.org/10.7554/eLife.27421.025>

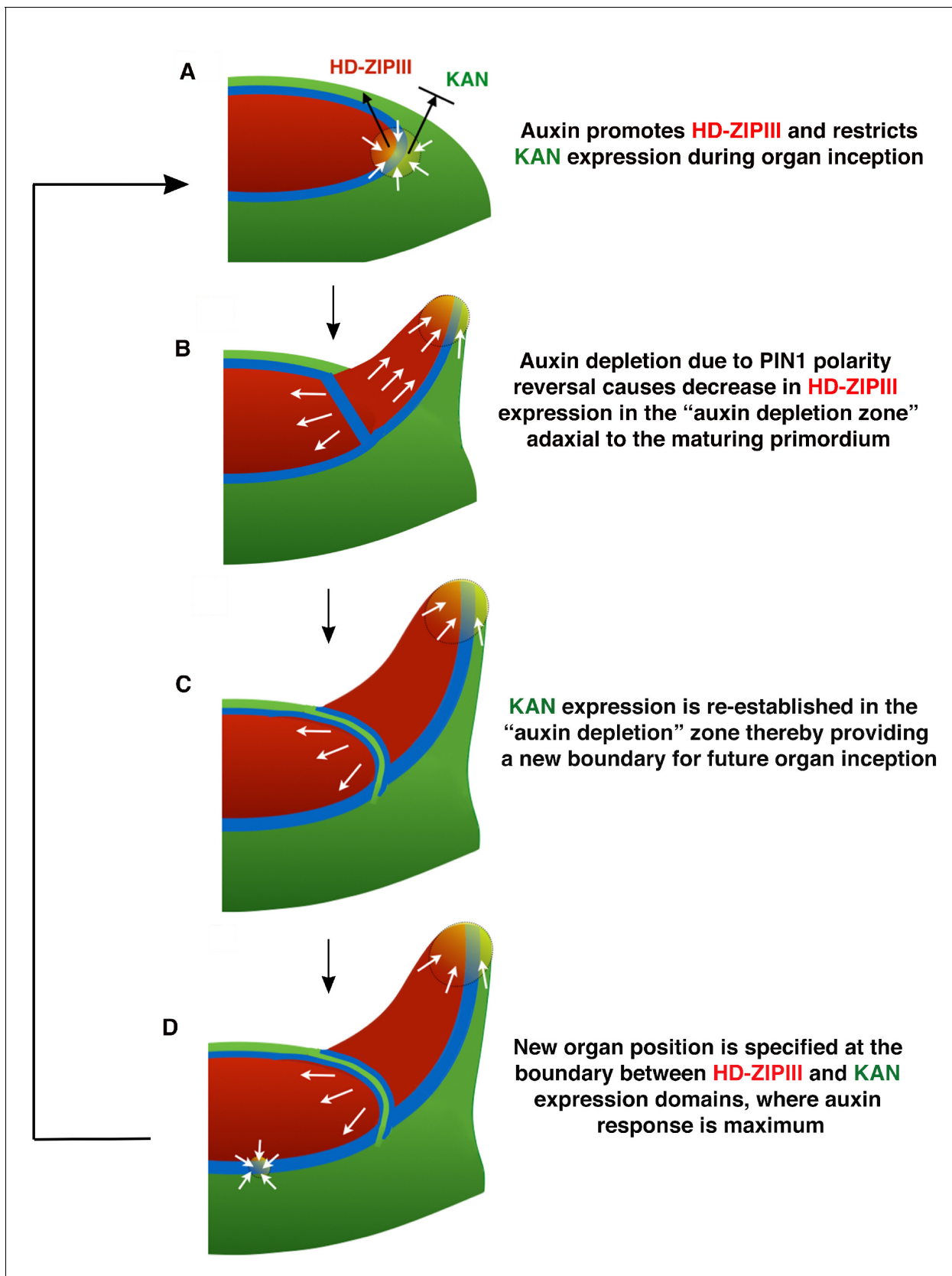


Figure 14. Conceptual Model. (A) During organ inception, PIN1 polarities (white arrows) and the alignment of microtubule arrays converge to create an auxin maximum and promote growth oriented towards the epidermal boundary between HD-ZIP III and KANADI (KAN) expression domains. As auxin
Figure 14 continued on next page

Figure 14 continued

accumulates, it promotes the expression of HD-ZIPIII thereby resulting in its extension towards the PIN1 convergence site. At the same time, auxin also prevents the acropetal expansion of KAN. Thus the boundary becomes fixed to the underlying cells. **(B)** As the primordium grows, PIN1 polarity in cells adaxial to the primordium reverse towards the meristem center and adjacent incipient primordia, thereby creating an auxin depletion zone leading to a reduction in HD-ZIPIII expression. **(C)** The reduction in auxin results in the re-establishment of KAN expression between the meristem and organ. **(D)** Auxin in the vicinity of the boundary in adjacent tissues leads to a localized transcriptional response that orients the polarity of surrounding cells into a convergence pattern, most likely via mechanical signals (*Bhatia et al., 2016*).

DOI: <https://doi.org/10.7554/eLife.27421.026>